astronomy

MDPI

Review

From a Dinuclear System to Close Binary Cosmic Objects

G. G. Adamian [1,*], N. V. Antonenko [1,2], H. Lenske [3] and V. V. Sargsyan [1,4]

[1] Joint Institute for Nuclear Research, 141980 Dubna, Russia; antonenk@theor.jinr.ru (N.V.A.); sargsyan@theor.jinr.ru (V.V.S.)
[2] Bogoliubov Laboratory of Theoretical Physics of Joint Institute of Nuclear Research, Tomsk Polytechnic University, 634050 Tomsk, Russia
[3] Institut für Theoretische Physik, Justus-Liebig-Universität, D-35392 Giessen, Germany; horst.lenske@physik.uni-giessen.de
[4] A. Alikhanyan National Science Laboratory (YerPhI), Yerevan 0036, Armenia
* Correspondence: adamian@theor.jinr.ru

Abstract: Applying the ideas from microscopic objects to macroscopic stellar and galactic systems, the evolution of compact di-stars and di-galaxies is studied in the mass asymmetry coordinate. The formation of stable binary systems is analyzed. The role of symmetrization of an initially asymmetric binary system is revealed in the transformation of gravitational energy into internal energy of stars or galaxies accompanied by the release of a huge amount of energy. For the contact binary stars, the change of the orbital period is explained by evolution to symmetry in mass asymmetry coordinates. The matter transfer in binary black holes is studied. The conditions for the merger of black holes in a binary system are analyzed regarding the radiation of gravitational waves. Using the model based on the Regge-like laws, the Darwin instability effect in binary systems is discussed. New analytical formulas are derived for the period of orbital rotation and the relative distance between the components of a binary system. The impossibility of the appearance of a binary cosmic object from a single cosmic object is revealed.

Keywords: close binary stars; close binary galaxies; mass asymmetry; fission

PACS: 95.30.-k; 26.90.+n

Citation: Adamian, G.G.; Antonenko, N.V.; Lenske, H.; Sargsyan, V.V. From a Dinuclear System to Close Binary Cosmic Objects. *Astronomy* **2023**, *2*, 58–89. https://doi.org/10.3390/astronomy2020006

Academic Editor: Ignatios Antoniadis

Received: 26 July 2022
Revised: 11 November 2022
Accepted: 29 March 2023
Published: 20 April 2023

1. Introduction

Di-star systems are widespread objects: about a quarter of all stars belong to the di-star family. Compact or close di-stars (binaries) with separation distances of only a few stellar diameters are of interest for stellar evolution, for example, for a merger process of stars. The distinctive feature of close binary systems is matter transfer (and ejection) [1–7], which is obviously impossible between two well-separated stars. A spectacular recent case is KIC 9832227, which attracted a lot of interest from the media when this binary star was predicted [8] to merge in 2022, which would lead to the formation of a red nova. Note that this has not happened yet. The luminous red novae have only recently been identified as a separate class of stellar transients [9]. They show up by relatively long outbursts with spectral distributions centered in the red, ranging in luminosities as intermediate between classical novae and supernovae. The luminous red nova V1309 Sco has played a key role. The Optical Gravitational Lensing Experiment (OGLE) revealed a shape of the light curve characteristic of a contact di-star with an exponentially decreasing orbital period [10]. These data well confirmed the previous prediction [11] that merging contact binary stars lead to luminous red novae.

The merger process is represented as *common-envelope* evolution [12,13]. Despite the short duration of this process, it has crucial consequences for stellar evolution. The binary components may survive with a reduced orbital separation, leading in some cases to compact binaries consisting of white dwarfs, neutron stars, and black holes. Some of these

systems can merge with the gravitational wave emission, as recently observed with the LIGO and Virgo interferometers [14]. Alternatively, the binary object can merge into a single one having exotic properties. There is a general opinion that the process of merger is an insufficiently studied problem of stellar evolution [8,15,16]. However, there is some consensus on the mechanisms of the important stages of contact binary evolution. Initial separations in a binary are large, with orbital periods of days to months. Interaction with the third star and the tidal friction may reduce the binary period to a day or two, as found in the dynamical simulations [17] and observations [18]. Both magnetic braking and internal structure evolution may bring the binary into contact. If this happens, the stellar radii and Roche geometry prevent further evolution of the orbital period, ending in a stellar merger. As found in ref. [11], red novae with a wide range of luminosities can result from contact di-stars with various initial masses.

As is commonly believed, contact binaries, for example, W UMa, end their evolution by merging into a single star [7]. The dissipation of orbital energy in the initial phase of merger led to the appearance of the glowing red nova V1309 Sco observed in 2008. However, the details of the matter transfer between the parts of the contact binary object or the mechanism triggering the merger are still unclear. The work [16] favors a gradual mass transfer from a less massive (with a smaller radius) secondary star to a primary one driven by the energy received from the primary. The contact is supported by the aforementioned magnetic braking or internal structure evolution. This results in an abrupt end when the mass ratio leads to the Darwin instability to start a merger which for a red nova seems to be the triggering mechanism for the outburst [10,19]. The Darwin instability occurs when the mass ratio becomes small enough, and the heavy star can no longer keep the light star synchronously rotating via tidal interaction. The orbital angular momentum transferred from the intrinsic spin changes the orbit more than the spin, which leads to a runaway. As found, for massive primary stars of the main sequence, this happens at a mass ratio of 0.09 [20]. There is also another scenario [21]: after contact of stars, there is a brief but intense mass transfer in a di-star system, changing the originally more massive star into a less massive one. This process may oscillate until a stable contact configuration is eventually achieved. A dynamic mass transfer without the Darwin instability was also investigated [22], and mergers triggered by a tidal runaway based on a non-equilibrium response to tidal dissipation [23] were considered. Thus, more detailed observational and theoretical studies are required.

Overcontact, contact, and near-contact binaries, forming di-star compounds with the average distances between the stars close to the sum of their radii [4–7] are of great interest in the study of stellar evolution. Information about the evolution of compact binaries is necessary to understand the processes observed in isolated stars. Compact binary stars are a good laboratory for a wide range of astrophysical phenomena, such as mass transfer between stars. The observations of their evolution verify our understanding of the inner structure of stars.

The problem of the origin of binary stars or binary galaxies is still unclear [4–7,24,25]. As shown in ref. [26], there is no dissociative equilibrium between single and binary stars in the galaxy. The number of binary stars is many orders of magnitude larger than expected for dissociative equilibrium. So the origin of binary stars is not related to the capture of one star by another into a bound orbit. In addition, there is no sharp difference between close and wide binary stars, and the angular momenta relative to their centers of gravity are extremely large. Angular momenta are in the interval between values close to the angular moments of stars with extremely high rotational velocity (close binary stars) and values exceeding these values by thousands of times (wide binary stars). These facts refute the assumption about the origin of binary stars due to the fission of individual stars. According to the law of conservation, the angular momentum of a binary star does not exceed the angular momentum of individual stars with extremely high rotational speeds. These conclusions are valid only if we ignore external influences on binary star evolution [26–28].

Since mass transfer is an important observable for close di-stars and di-galaxies, it is meaningful to study the evolution of the system in the mass asymmetry coordinate $\eta = (M_1 - M_2)/(M_1 + M_2)$, where M_i $(i = 1, 2)$ are the masses of the components of the binary system at fixed total mass $M = M_1 + M_2$ and orbital angular momentum L of the system. Classical Newtonian mechanics can be used to explore the evolution of close binary stars and galaxies in their center-of-mass coordinate system by analyzing the total potential energy as a function of η [29–35]. The limits of the formation and evolution of binary systems are of interest. The methods used were tested for similar processes in nuclear systems where mass asymmetry is an important collective coordinate governing the fusion of two nuclei [36,37]. A nuclear molecule or a dinuclear system consists of two individual touching nuclei. There are two main collective degrees of freedom in a dinuclear system which govern its dynamics: (i) the relative motion between the clusters leading to quasistationary states in the internuclear potential and to the decay into two fragments which is called quasifission since no compound system is first formed, (ii) the transfer of nucleons or light particles between two clusters of the dinuclear system leading to evolution in mass and charge asymmetries. There is a structural forbiddenness for the motion of the nuclei to smaller internuclear distances during the fusion process. Fusion of heavy nuclei in the internuclear distance R is impossible and can occur due to the transfer of nucleons, i.e., by a motion in η [36,37].

Nuclear dynamics is certainly different from the gravitational interactions of di-stars and di-galaxies. Nuclear reactions are governed by short-range strong interactions, onto which minor contributions of long-range (repulsive) Coulomb and centrifugal forces are superimposed. The dinuclear approach is a key tool for describing the fusion of two heavy nuclei. In the approaching phase and after fusion, there is a mass loss by the emission of protons, neutrons, and light clusters like Alpha particles. Once a critical distance and mass ratio are reached, fusion occurs. A highly excited compound nucleus is formed in thermal equilibrium at temperatures of the order of one to a few MeV, corresponding to 10^7 K, cooled down rapidly by ejection of nucleons, nuclear clusters, and $\gamma-$quanta. Hence, dinuclear dynamics covers essentially the same spectrum of phenomena as expected for di-stars and di-galaxies. Thus, it is worth exploring to what extent the method from the femtoscale of microscopic objects is applicable to macroscopic binary galactic and stellar systems [29–35].

2. Theoretical Approach

The differential of the total energy of a binary stellar or galactic system is expressed as a function of relative distance $\mathbf{r}$, conjugate canonical momentum $\mathbf{p}$, and mass asymmetry coordinate η as

$$dE(\mathbf{r}, \mathbf{p}, \eta) = \frac{\partial E}{\partial t} dt + \frac{\partial E}{\partial \mathbf{r}} d\mathbf{r} + \frac{\partial E}{\partial \mathbf{p}} d\mathbf{p} + \frac{\partial E}{\partial \eta} d\eta. \quad (1)$$

As we consider the binary system as a closed system, the conservation of the total energy results in

$$\frac{\partial E}{\partial \eta} \frac{d\eta}{dt} = 0 \quad (2)$$

where $\partial E/\partial \eta = 0$ is the general solution. In the center of the mass system, the total energy of the binary system is a sum of radial and orbital parts of kinetic energies and potential energy. As seen below, we attach the orbital kinetic energy part to the interaction V between two components of the binary system. In this case, the expression of the total energy of the di-star system reads as

$$E = \frac{p_r^2}{2\mu} + U, \quad (3)$$

where p_r is the radial component of the momentum $\mathbf{p}$ and $\mu = \mu(\eta) = M_1M_2/M = M(1-\eta^2)/4$ is the reduced mass.

The total potential energy of a binary stellar or galactic system,

$$U = U_1 + U_2 + V, \tag{4}$$

is the sum of the potential energies

$$U_k = -\omega_k \frac{GM_k^2}{2R_k}, \tag{5}$$

of its components ($k = 1, 2$), and the energy V of their interaction. The radiation energy is much smaller than the absolute values of $U_{1,2}$ and V to be disregarded. In Equation (5), G, ω_k, M_k, and R_k are, respectively, the gravitational constant, the dimensionless structural factor, the mass, and the radius of the component. In general, the value of ω_k is determined by the density profile of a stellar or a galactic object. By employing the relation known from observations, we express the radius of the object in terms of its mass as [29,30]

$$R_k = \frac{1}{g} M_k^n$$

where n and g are the constants. So

$$U_k = -\frac{Gg\omega_k M_k^{2-n}}{2}. \tag{6}$$

Since two objects rotate around the common center of mass, the star–star interaction potential contains, together with the gravitational energy of interaction V_G, the kinetic energy of orbital rotation V_R:

$$V(r) = V_G + V_R = V_G + \frac{L^2}{2\mu r^2}, \tag{7}$$

where L is the orbital angular momentum of the binary system, which is conserved during the conservative mass transfer. At $r \geq r_t = R_1 + R_2$ and $r \leq r_t$,

$$V_G(r) = -\frac{GM_1M_2}{r} \tag{8}$$

and

$$V_G(r) = -\frac{GM_1M_2}{2r_t}\left[3 - \frac{r^2}{r_t^2}\right], \tag{9}$$

respectively [38]. Here, r_t is the touching distance. From the conditions $\partial V/\partial r|_{r=r_m} = 0$ and $\partial^2 V/\partial r^2|_{r=r_m} > 0$, we find the equilibrium relative distance between two objects corresponding to the minimum of V:

$$r_m = \frac{L^2}{G\mu^2 M} \tag{10}$$

at $r_m \geq r_t$ and

$$r_m = \left(\frac{L^2 r_t^3}{G\mu^2 M}\right)^{1/4} \tag{11}$$

at $r_m < r_t$. Finally, one can derive the expression for the object–object interaction potential

$$V(r_m) = -\frac{GM_1M_2}{2r_m} = -\frac{G}{2}\omega_V M_1^3 M_2^3 \tag{12}$$

at $r_m \geq r_t$ or

$$V(r_m) = -\frac{GM_1M_2}{2r_t}\left[3 - \frac{2r_m^2}{r_t^2}\right] = -\frac{G}{2}\frac{gM_1M_2}{M_1^n + M_2^n}\left[3 - \frac{2g^2}{\omega_V^2 M_1^4 M_2^4 (M_1^n + M_2^n)^2}\right] \tag{13}$$

at $r_m < r_t$. Here,

$$\omega_V = \frac{1}{M^2 \mu_i^2 r_{mi}}$$

and r_{mi} and $\mu_i = \mu(\eta_i) = \frac{M_{1i}M_{2i}}{M} = \frac{M}{4}(1 - \eta_i^2)$ are, respectively, the distance between its components and the reduced mass of the initial binary system. Deriving Equations (12) and (13), we employ the known relation

$$r_m = \left(\frac{\mu_i}{\mu}\right)^2 r_{mi}. \tag{14}$$

Using Equations (6), (12) and (13), we obtain the final expression for the total potential energy (4) of the binary system

$$U = -\frac{G}{2}\left(g[\omega_1 M_1^{2-n} + \omega_2 M_2^{2-n}] + \omega_V M_1^3 M_2^3\right) \tag{15}$$

at $r_m \geq r_t$ and

$$U = -\frac{G}{2}g\left(\omega_1 M_1^{2-n} + \omega_2 M_2^{2-n} + \frac{M_1M_2}{M_1^n + M_2^n}\left[3 - \frac{2g^2}{\omega_V^2 M_1^4 M_2^4 (M_1^n + M_2^n)^2}\right]\right) \tag{16}$$

at $r_m < r_t$.

For the binary systems considered, the velocity $v_r(r_m) \ll c$, where c is the speed of light; therefore, the relativistic effects can be ignored. Since $GM_k/r_m \ll c^2$, the gravitational field is rather weak, and the equations of Newtonian mechanics can be used instead of the equations of general relativity. Note that exotic binary systems with neutron stars, white dwarfs, and black holes are not considered in this section.

2.1. Binary Stars

In order to calculate the factor ω_k, we make use of the single-star model from ref. [6], because it describes well the observed relations between the temperature, radius, mass, and luminosity of stars; the mass distribution of stars; magnetic fields of stars; spectra of seismic vibrations of the Sun; and other features of stars. Employing the dimensionless structure factor

$$\omega_k = 1.644\left(\frac{M_\odot}{M_k}\right)^{1/4} \tag{17}$$

from [6], the observed radius-mass relation ($n = 2/3$)

$$R_k = \frac{1}{g}M_k^{2/3} = R_\odot\left(\frac{M_k}{M_\odot}\right)^{2/3},$$

and the relation between the star masses $M_1 = \frac{M}{2}(1 + \eta)$ and $M_2 = \frac{M}{2}(1 - \eta)$ in the binary system and the mass asymmetry coordinate η, we find from Equations (15) and (16) that

$$U = -\frac{GM_\odot^2}{2R_\odot}\left(\alpha[(1 + \eta)^{13/12} + (1 - \eta)^{13/12}] + \beta[1 - \eta^2]^3\right) \tag{18}$$

at $r_m \geq r_t$ and

$$U = -\frac{GM_\odot^2}{2R_\odot}\Big(\alpha[(1+\eta)^{13/12}+(1-\eta)^{13/12}] + \beta_1\frac{1-\eta^2}{(1+\eta)^{2/3}+(1-\eta)^{2/3}}\left[3-\frac{\gamma}{[1-\eta^2][(1+\eta)^{2/3}+(1-\eta)^{2/3}]^{1/2}}\right]\Big) \quad (19)$$

at $r_m < r_t$, where

$$\alpha = 1.644\left(\frac{M}{2M_\odot}\right)^{13/12},$$

$$\beta = \frac{GM^5R_\odot}{64L_i^2M_\odot^2} = \frac{GM_\odot^3R_\odot}{2L_i^2}\left(\frac{M}{2M_\odot}\right)^5,$$

$$\beta_1 = \left(\frac{M}{2M_\odot}\right)^{4/3},$$

$$\gamma = \frac{2^{10/3}L_iM_\odot^{1/3}}{\left(GR_\odot M^{11/3}\right)^{1/2}}.$$

Here, we assume that the orbital angular momentum L_i and total mass M are conserved during the evolution of a di-star in the mass asymmetry coordinate η. The orbital angular momentum L_i is calculated by using the observed masses $M_{k,i}$ of stars and period $P_{\mathrm{orb},i}$ of their orbital rotation [39–43].

As seen from Equation (18), the stability of a binary stellar system depends on the orbital-rotation period $P_{\mathrm{orb},i}$ or on the value of $L_i = \mu_i(GMr_{mi})^{1/2} = \mu_i\left(G^2M^2P_{\mathrm{orb},i}/(2\pi)\right)^{1/3}$ and total mass M. Employing Equation (18), we can study the evolution of a binary stellar system in η. The extremes of the potential energy are determined from the numerical solution of the equation

$$\frac{\partial U}{\partial \eta} = -\frac{GM_\odot^2}{2R_\odot}\left(\frac{13}{12}\alpha[(1+\eta)^{1/12}-(1-\eta)^{1/12}]-6\beta\eta[1-\eta^2]^2\right) = 0. \quad (20)$$

As follows, $\eta = \eta_m = 0$ (symmetric binary system) is the root of Equation (20) and at $\eta = 0$ the potential has a minimum if

$$\alpha < \alpha_{cr} = \frac{432}{13}\beta$$

or

$$P_{\mathrm{orb},i} < \frac{128.5\pi}{(1-\eta_i^2)^3}\left(\frac{R_\odot^3}{GM_\odot}\right)^{1/2}\left(\frac{M}{2M_\odot}\right)^{7/8}$$

and a maximum if $\alpha > \alpha_{cr}$. The minimum at $\eta = 0$ lies symmetrically relative to the two barriers at $\eta = \pm\eta_b$. Expanding Equation (20) up to the third-order terms in η and solving it, the barrier positions are obtained as

$$\eta_b = 2^{-1/2}\left(\frac{864^2\beta - 22464\alpha}{864^2\beta + 3289\alpha}\right)^{1/2}.$$

So at $\alpha < \alpha_{cr}$ the potential energy as a function of η has two symmetric maxima at $\eta = \pm\eta_b$ and the minimum at $\eta = \eta_m = 0$. The fusion of two stars with $|\eta_i| < \eta_b$ occurs only by overcoming the barrier at $\eta = +\eta_b$ or $\eta = -\eta_b$. With decreasing ratio α/β, the value of $B_\eta = U(\eta_b) - U(\eta_i)$ increases and the symmetric di-star system becomes more stable. The evolution of two stars with $0 < |\eta_i| < \eta_b$ to the symmetric di-star configuration is energetically favorable. Thus, an initially asymmetric binary system with $|\eta| = |\eta_i| < \eta_b$ is driven to mass symmetry, implying a flow of mass towards equilibrium and an increase in internal energy of stars by the amount $\Delta U = U(\eta_i) - U(\eta = 0)$ (Figure 1a). At $\alpha \geq \alpha_{cr}$,

$\eta_m = \eta_b = 0$ and the inverse U-type potential has a maximum at $\eta = 0$. In such a system, the fusion of stars (one star "swallows" another) is the only mode of motion in η transforming the di-star into a mono-star with the release of energy $E_f = U(\eta_i) - U(\eta = 1)$ (Figure 1b).

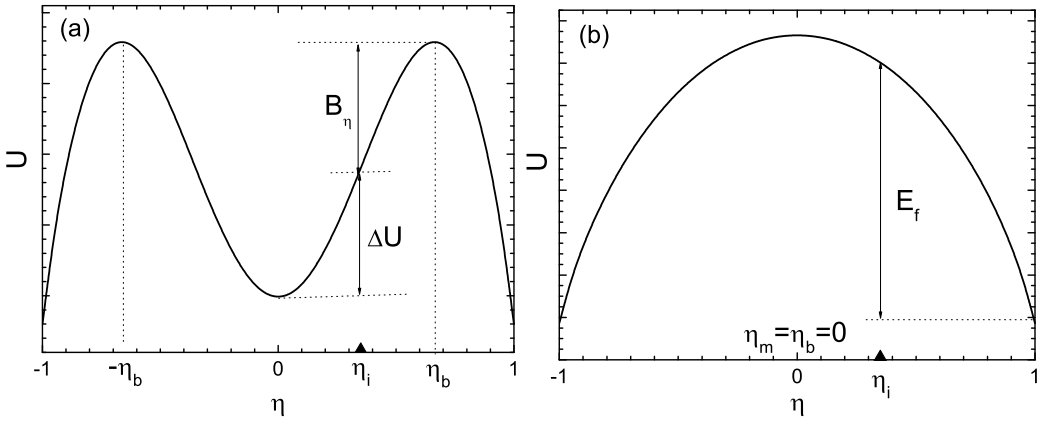

Figure 1. The schematic driving potential energies of the star–star systems at $\alpha < \alpha_{cr}$ (**a**), and $\alpha > \alpha_{cr}$ (**b**). The arrows show the corresponding initial binary stars. The notation used in the text is indicated.

If $\beta \gg \frac{1}{66}\alpha$, then $\eta_b \to 2^{-1/2} \approx 0.71$. In this case, the condition $0 < \eta_b < 2^{-1/2}$ means that an asymmetric system with the mass ratio $M_1/M_2 > (1 + 2^{1/2})^2 \approx 6$ moves to more asymmetric configurations and the relative distances between its components increase in accordance with Equation (11). These unstable binary stars with $|\eta| > \eta_b$ are unlikely to live long. Indeed, close binary stars with a high mass ratio are very rare objects (Figure 2). Note that this constraint on the mass ratio is independent of the relation used between the mass and the radius of the object.

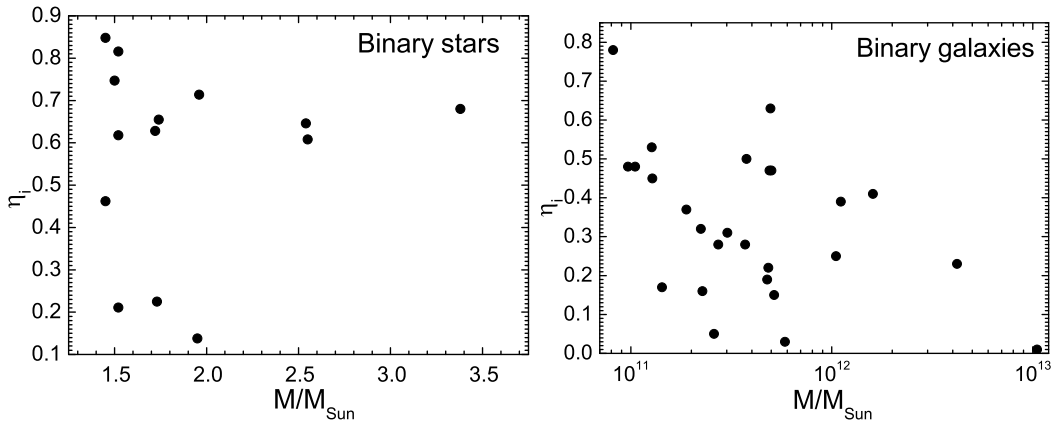

Figure 2. Mass asymmetry η_i versus the total mass $M/M_\odot = (M_{1i} + M_{2i})/M_\odot$ ($M_{\rm Sun} = M_\odot$) for the di-stars and di-galaxies from Tables 1–4.

Table 1. Calculated ($n = 2/3$) values of $|\eta_i|$, $\Delta U = U(\eta_i) - U(\eta = 0)$, $B_\eta = U(\eta_b) - U(\eta_i)$, $B_f = U(\eta_b) - U(\eta = 1)$, and data from observations on $M_1/M_\odot$, $M_2/M_\odot$, P_{orb} [8,42,43] for the close binary stars (BS) listed.

BS	$\frac{M_1}{M_\odot}$	$\frac{M_2}{M_\odot}$	$\lvert\eta_i\rvert$	P_{orb} (Days)	ΔU (J)	B_η (J)	B_f (J)
AH Aur	1.68	0.28	0.71	0.4941	10^{41}	2×10^{40}	8×10^{39}
AP Aur	2.05	0.50	0.61	0.5694	10^{41}	3×10^{40}	10^{40}
DN Aur	1.44	0.30	0.66	0.6169	8×10^{40}	10^{40}	9×10^{39}
AW Vir	1.11	0.84	0.14	0.3540	4×10^{39}	4×10^{40}	10^{40}
AW UMa	1.38	0.14	0.82	0.4387	10^{41}	7×10^{39}	5×10^{39}
HV UMa	2.84	0.54	0.68	0.7108	2×10^{41}	3×10^{40}	2×10^{40}
KIC9832227	1.40	0.32	0.63	0.4583	7×10^{40}	2×10^{40}	9×10^{39}
HV Aqr	1.31	0.19	0.75	0.3734	9×10^{40}	10^{40}	6×10^{39}
QX And	1.23	0.29	0.62	0.4122	6×10^{40}	10^{40}	8×10^{39}
RR Cen	2.09	0.45	0.65	0.6060	10^{41}	2×10^{40}	10^{40}
EM Lac	1.06	0.67	0.23	0.3891	7×10^{39}	3×10^{40}	10^{40}
GW Cep	1.06	0.39	0.46	0.3188	3×10^{40}	2×10^{40}	8×10^{39}
V700 Cyg	0.92	0.60	0.21	0.3400	6×10^{40}	3×10^{40}	10^{40}
V870 Ara	1.34	0.11	0.85	0.3997	7×10^{40}	5×10^{40}	4×10^{39}

Table 2. The calculated ($n = 2/5$) values of $|\eta_i|$, $\Delta U = U(\eta_i) - U(\eta = 0)$, $B_\eta = U(\eta_b) - U(\eta_i)$, and $B_f = U(\eta = \eta_b) - U(\eta = 1)$ and observational data (ordinal numbers and morphological types Ty of galaxies according to Hubble's classification, total orbital mass $M/M_\odot$ of pairs in Sun's mass units, projection of the linear distance X between the components, and linear diameters $A_{25}(1i) = 2R_{1i}$ and $A_{25}(2i) = 2R_{2i}$ of the components) of close binary elliptical galaxies (BG) from the catalog of isolated galaxy pairs [24].

BG	Ty	$\frac{M}{M_\odot}$	X (kpc)	$A_{25}(1i)$ (kpc)	$A_{25}(2i)$ (kpc)	$\lvert\eta_i\rvert$	ΔU (J)	B_η (J)	B_f (J)
194	E-E	2.72×10^{11}	27.0	36.9	29.3	0.28	2×10^{50}	2×10^{50}	3×10^{51}
279	E-E	3.76×10^{11}	20.6	27.2	17.5	0.50	3×10^{51}	2×10^{50}	6×10^{51}
399	E-E	5.84×10^{11}	28.2	27.1	26.5	0.03	3×10^{48}	2×10^{50}	2×10^{52}
501	E-E	1.05×10^{13}	38.3	36.0	35.7	0.01	10^{50}	3×10^{52}	4×10^{54}
554	E-E	1.05×10^{12}	57.6	52.2	42.7	0.25	2×10^{50}	2×10^{48}	3×10^{52}
577	E-E	2.27×10^{11}	21.3	29.0	25.5	0.16	6×10^{49}	2×10^{50}	3×10^{51}

Table 3. The same as in Table 2 but for other close binary elliptic-spiral galaxies.

BG	Ty	$\frac{M}{M_\odot}$	X (kpc)	$A_{25}(1i)$ (kpc)	$A_{25}(2i)$ (kpc)	$\lvert\eta_i\rvert$	ΔU (J)	B_η (J)	B_f (J)
144	E-Sa	1.43×10^{11}	17.1	18.3	16.0	0.17	3×10^{49}	3×10^{49}	2×10^{51}
254	E-Sb	5.16×10^{11}	47.7	48.9	43.3	0.15	6×10^{49}	8×10^{49}	8×10^{51}
331	SO-E	8.15×10^{10}	17.4	23.4	10.1	0.78	2×10^{51}	3×10^{48}	2×10^{50}
552	Sa-E	5.01×10^{11}	38.8	39.5	26.2	0.47	3×10^{50}	6×10^{48}	9×10^{51}

Table 4. The same as in Table 2 but for close binary spiral galaxies.

BG	*Ty*	$\frac{M}{M_\odot}$	X (kpc)	$A_{25}(1i)$ (kpc)	$A_{25}(2i)$ (kpc)	$\lvert\eta_i\rvert$	ΔU (J)	B_η (J)	B_f (J)
1	Sb-Sb	3.70×10^{11}	9.3	12.1	11.8	0.28	2×10^{50}	6×10^{50}	10^{52}
105	Sb-Sb	1.89×10^{11}	23.5	28.8	21.2	0.37	2×10^{50}	5×10^{49}	2×10^{51}
165	Sa-Sb	2.23×10^{11}	10.0	12.9	9.9	0.32	5×10^{50}	2×10^{50}	5×10^{50}
201	Sa-Sb	1.05×10^{11}	32.5	34.8	22.8	0.48	9×10^{49}	10^{48}	4×10^{50}
206	Sb-Sb	1.28×10^{11}	16.8	13.2	9.0	0.45			2×10^{51}
237	Sb-Sb	4.20×10^{12}	46.3	42.9	35.7	0.23	5×10^{51}	4×10^{50}	8×10^{53}
243	Sb-SO	3.02×10^{11}	37.6	28.1	21.7	0.31			5×10^{51}
272	Sc-Sc	1.11×10^{12}	83.5	32.7	23.6	0.39			8×10^{52}
297	Sc-Sc	1.27×10^{11}	29.4	29.9	18.7	0.53	2×10^{50}	10^{47}	7×10^{50}
439	Sa-SO	4.95×10^{11}	29.4	23.4	13.0	0.63			10^{52}
474	Sa-Sb	4.77×10^{11}	21.7	27.1	23.3	0.19	3×10^{50}	6×10^{50}	10^{52}
490	Sa-Sa	4.90×10^{11}	30.0	29.6	19.6	0.47	2×10^{51}	6×10^{47}	10^{52}
507	Sb-Sa	1.60×10^{12}	32.2	35.5	25.1	0.41	10^{52}	8×10^{50}	10^{53}
516	Sc-Sb	2.59×10^{11}	20.0	21.1	20.3	0.05	4×10^{48}	9×10^{49}	4×10^{51}
524	Sb-Sc	4.83×10^{11}	15.9	17.4	14.6	0.22	4×10^{50}	3×10^{50}	2×10^{52}
539	SO-Sa	9.68×10^{10}	17.8	25.8	17.0	0.48	2×10^{50}	3×10^{49}	4×10^{50}

2.2. Binary Galaxies

Employing $\omega_k = 1$ for the dimensionless structural factor, the radius-mass relation ($n = 2/5$) [24]

$$R_k = \frac{1}{g} M_k^{2/5} = \left(R_{1i}^{5/2} + R_{2i}^{5/2}\right)^{2/5} \left(\frac{M_k}{M}\right)^{2/5},$$

observed for the galaxies of large mass ($M_{1i,2i} > 10^{10} M_\odot$), where $M_{1i,2i}$ and $R_{1i,2i} = \frac{1}{g} M_{1i,2i}^{2/5}$ are, respectively, the masses and radii of the components of the binary system before transferring the mass, and the relation between the coordinate η and the galaxy masses M_1 and M_2 in the binary system, we write Equations (15) and (16) as

$$U = -\alpha[(1+\eta)^{8/5} + (1-\eta)^{8/5}] - \beta[1-\eta^2]^3 \tag{21}$$

at $r_m \geq r_t$ and

$$\begin{aligned} U &= -\alpha\left[(1+\eta)^{8/5} + (1-\eta)^{8/5} + \frac{3(1-\eta^2)}{(1+\eta)^{2/5} + (1-\eta)^{2/5}}\right] \\ &+ \frac{\beta_1}{[1-\eta^2][(1+\eta)^{2/5} + (1-\eta)^{2/5}]^3} \end{aligned} \tag{22}$$

at $r_m < r_t$, where

$$\alpha = \frac{GM^2}{2^{13/5}\left(R_{1i}^{5/2} + R_{2i}^{5/2}\right)^{2/5}},$$

$$\beta = \frac{GM^2\left(R_{1i}^{5/2} + R_{2i}^{5/2}\right)^4}{128 r_{mi} R_{1i}^5 R_{2i}^5},$$

$$\beta_1 = \frac{2^{36/5} G \mu_i^4 r_{mi}^2}{M^2\left(R_{1i}^{5/2} + R_{2i}^{5/2}\right)^{6/5}}.$$

In order to calculate α and β, the observed values of M, R_{1i}, R_{2i}, and $r_{mi} = \frac{\pi}{4} X$ are used, where X is the projection of the linear distance between the components of the binary

galaxy from ref. [24]. The potential energy has an extremum at $\eta = \eta_m = 0$; it is the minimum if

$$\alpha < \alpha_{cr} = \frac{25}{8}\beta$$

or

$$r_{mi} < \frac{25\left(R_{1i}^{5/2} + R_{2i}^{5/2}\right)^{22/5}}{2^{37/5}R_{1i}^5 R_{2i}^5}$$

and the maximum if $\alpha > \alpha_{cr}$. As readily seen, the extreme points of the potential depend only on r_{mi} and $R_{1i,2i}$. Note that for touching binary systems ($r_{mi} \approx R_{1i} + R_{2i}$) there is a symmetric minimum because the condition

$$\alpha < \frac{25}{8}\beta$$

or

$$\frac{25\left(R_{1i}^{5/2} + R_{2i}^{5/2}\right)^{22/5}}{16\left(4R_{1i}^{5/2}R_{2i}^{5/2}\right)^{11/5}} > 1$$

always holds. Expanding the equation $\frac{\partial U}{\partial \eta} = 0$ to the third-order terms in η inclusive and solving it, we find the barrier positions at

$$\eta_b = \pm 2^{-1/2}\left(\frac{1875\beta - 600\alpha}{1875\beta + 28\alpha}\right)^{1/2} \approx \pm 2^{-1/2}\left[1 - \frac{2^{37/5}r_{mi}R_{1i}^5 R_{2i}^5}{25\left(R_{1i}^{5/2} + R_{2i}^{5/2}\right)^{22/5}}\right]^{1/2} \quad (23)$$

($\alpha < \alpha_{cr}$). As a result, $\eta_b < 2^{-1/2} \approx 0.71$. So, in a strongly asymmetric binary system with the mass ratio $M_{1i}/M_{2i} > (1 + 2^{1/2})^2 \approx 6$, the galaxies should fly apart. Indeed, the binary galaxies with a high mass ratio are rare objects [24] (Figure 2).

3. Mass Transfer in Close Binary Cosmic Systems as a Source of Energy in the Universe

3.1. Close Binary Stars

As assumed, the values of L_i and M are conserved during the binary star evolution in η. The orbital angular momentum L_i is found using the observed star masses $M_{1i,2i}$ and period $P_{orb,i}$ of orbital rotation at $\eta = \eta_i$. The binary stars differ in values of M and L_i and, accordingly, have potential energies of a different kind.

One can express the potential energy (18) in units of

$$u = u_1 + u_2 + xv = (1 + \eta)^{13/12} + (1 - \eta)^{13/12} + x(1 - \eta^2)^3,$$

where $x = \frac{GM_\odot^3 R_\odot}{3.288L_i^2}\left(\frac{M}{2M_\odot}\right)^{47/12}$. As seen from Figure 3, at relatively large $x > 0.025$ the u as a function of η has two asymmetric maxima and the minimum at $\eta = 0$. The decrease in x causes the change of the shape of potential energy in η: η_b approaches $\eta_m = 0$ and the height of barrier B_η in η decreases. At x = 0.025, there is an inverse U-type symmetric potential with a maximum at $\eta = 0$, and the di-star system becomes unstable with respect to the mass transfer coordinate. The asymmetrization of the system becomes energetically favorable. The parameter $x \sim M^{47/12}/L_i^2$ depends on M and L_i. For example, the value of x decreases with increasing L_i or decreasing M.

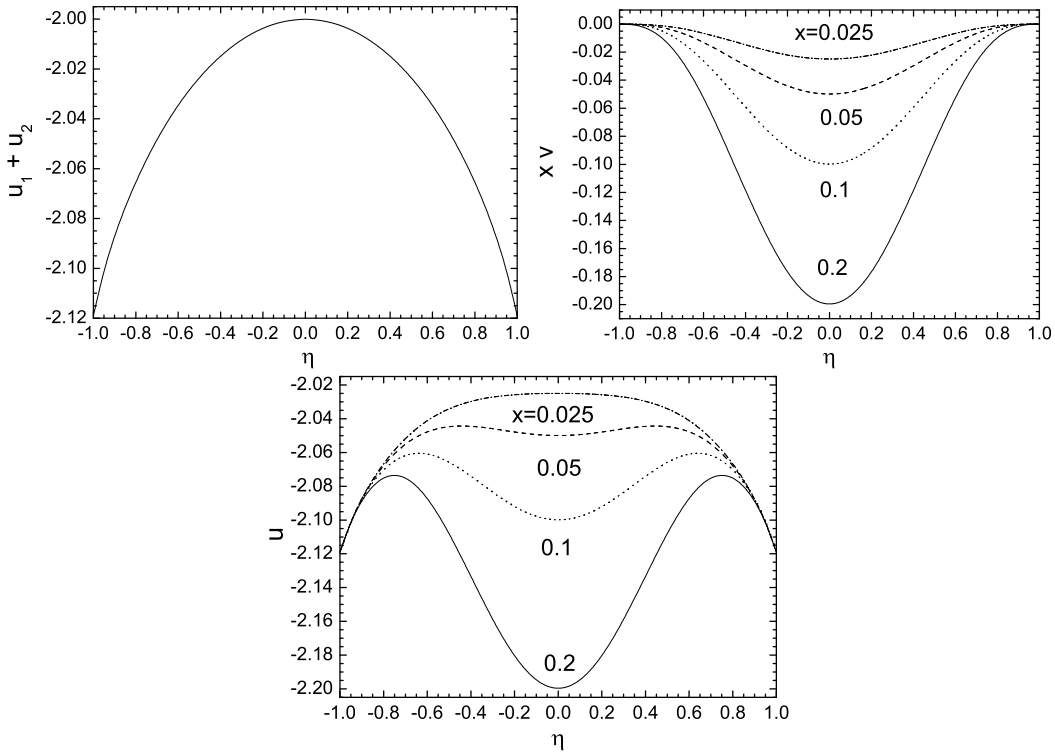

Figure 3. The calculated dimensionless u, $u_1 + u_2$, and xv vs. η at indicated x (see text).

In Figures 4–6, the potential energies (driving potentials) $U(\eta)$ versus η are presented for the close di-star systems. For the systems considered, $\alpha < \alpha_{cr}$ or

$$L_i < [10.1GR_{\odot}M_{\odot}^3]^{1/2}\left(\frac{M}{2M_{\odot}}\right)^{47/24},$$

and the potential energies have symmetric barriers at $\eta = \pm\eta_b$ and a minimum at $\eta = \eta_m = 0$. As seen in Figure 4, the barrier in η appears as a result of the interplay between the gravitational energy $U_1 + U_2$ of the stars and the star–star interaction V. Both energies have a different trend as a function of η: $U_1 + U_2$ decreases and V increases with changing η from $\eta = 0$ to ± 1. One should note that the driving potentials $U(\eta)$ for the di-star systems look similar to the driving potentials for the microscopic dinuclear systems [36,37]. The same conclusion was derived in ref. [29] with the η-independent (constant) structural factors ω_i.

The evolution of the di-star system depends on its initial mass asymmetry $\eta = \eta_i$. If the original di-star is asymmetric and $|\eta_i| < |\eta_b|$, then it evolves in η to the global minimum at $\eta = 0$ (a symmetric di-star system). The matter of a heavy star moves to an adjacent light star enforcing the symmetrization of a di-star without additional driving energy. The symmetrization of an asymmetric binary star is accompanied by the decrease of potential energy U or the transformation of the potential energy into the internal energy of stars. A huge amount of energy $\Delta U \approx 10^{39} - 10^{41}$ J is released during the symmetrization (see Figures 5 and 6 and Table 1). So the symmetric di-star is created at large excitation energy. Note that for the binary stars considered, the energy of a single star ($|\eta| = 1$) is larger than the energy of a symmetric binary ($\eta = 0$). So the merger of stars in a di-star is energetically unfavorable.

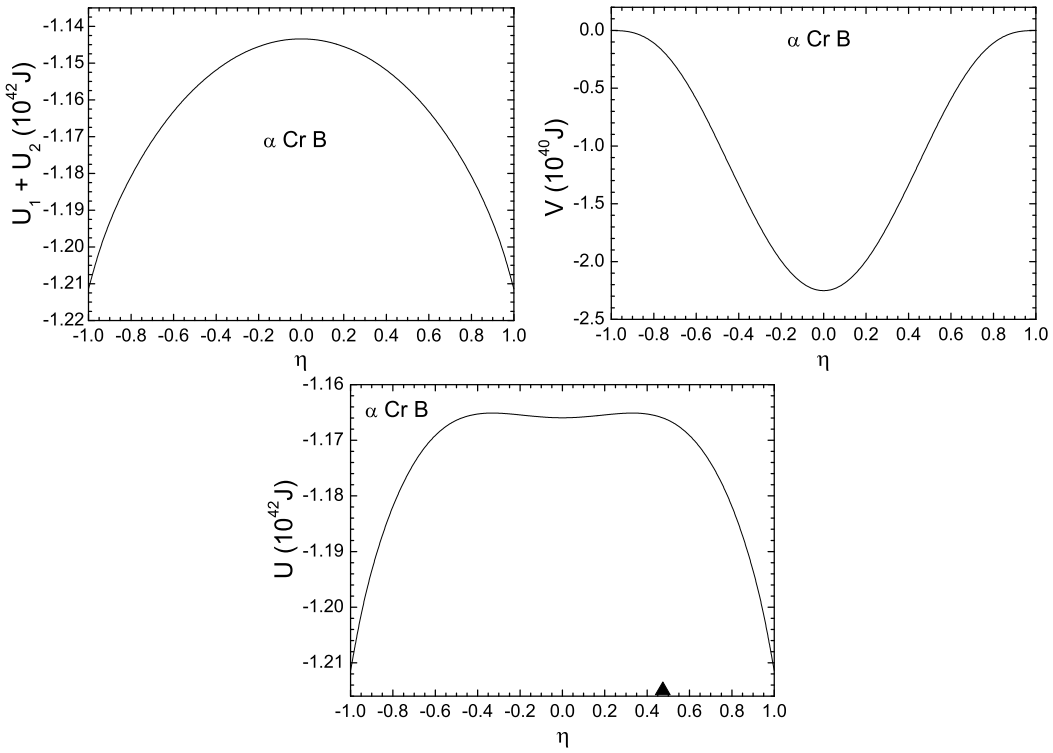

Figure 4. Calculated gravitational energies $U_1 + U_2$ of the stars; the energy of interaction V between them; the total potential energy U versus the mass-asymmetry coordinate η for the close binary star α Cr B. The arrow indicates the value of η_i for the original binary system.

When the symmetrization of a binary occurs, the distance between the stars decreases because of the increase in the gravitational interaction. After a symmetric di-star is formed, it performs zero-point oscillations near $\eta = 0$, which cause the radiation of gravitational waves. The transfer of matter in the symmetric di-stars is a mass asymmetry fluctuation near $\eta = 0$. If there is a transmission (fluctuation) in one direction, then there is a transmission in the opposite direction, as proposed in ref. [21]. There are indications of that effect [7].

If $|\eta_i| > \eta_b$ or $\eta_b = 0$, the di-star system is unstable with respect to the asymmetrization. The matter is transferred from the light star to the heavy one even without additional external energy. We only know one close binary system α Cr B ($M_1 = 2.58M_\odot$, $M_2 = 0.92M_\odot$, $\omega_1 = 1.30$, $\omega_2 = 1.68$, $\beta/\alpha = 0.039$), for which $|\eta_i| = 0.47 > \eta_b = 0.33$ (Figure 4).

Since the fusion barriers B_η in η are quite large in Table 1 for the systems with $|\eta_i| < \eta_b$, there is a strong hindrance to the formation of a single star from the di-star system due to thermal diffusion in η. The existence of a barrier in η may be the reason why very asymmetric close di-stars with $|\eta_i| > \eta_b$ are rarely observed. Indeed, there can not be a stable di-star with a very light star, $|\eta_i| > \eta_b$.

A spectacular recent case is KIC 9832227, which was predicted [8] to be merged in 2022, enlightening the sky as a red nova. For this system ($\eta_i = 0.63$, $\eta_b = 0.84$), we conclude that a fast merger is excluded (see Figure 5). Instead, the di-star is driven towards mass symmetry. Matter is transferring from a heavy star to a light one, and the relative distance between two stars and the period of the orbital rotation decreases. A huge amount of energy $\Delta U \approx 10^{41}$ J is released during the symmetrization. As seen in Figure 5 and Table 1, the di-stars KIC 9832227 and RR Cen ($\eta_i = 0.65$, $\eta_b = 0.85$) have almost the same η_i, η_b, and potential energy dependencies on η. So the observation of the RR Cen di-star for a possible merger is also desirable. Observational data in ref. [44] refute the prediction for the 2022 red nova merger [8].

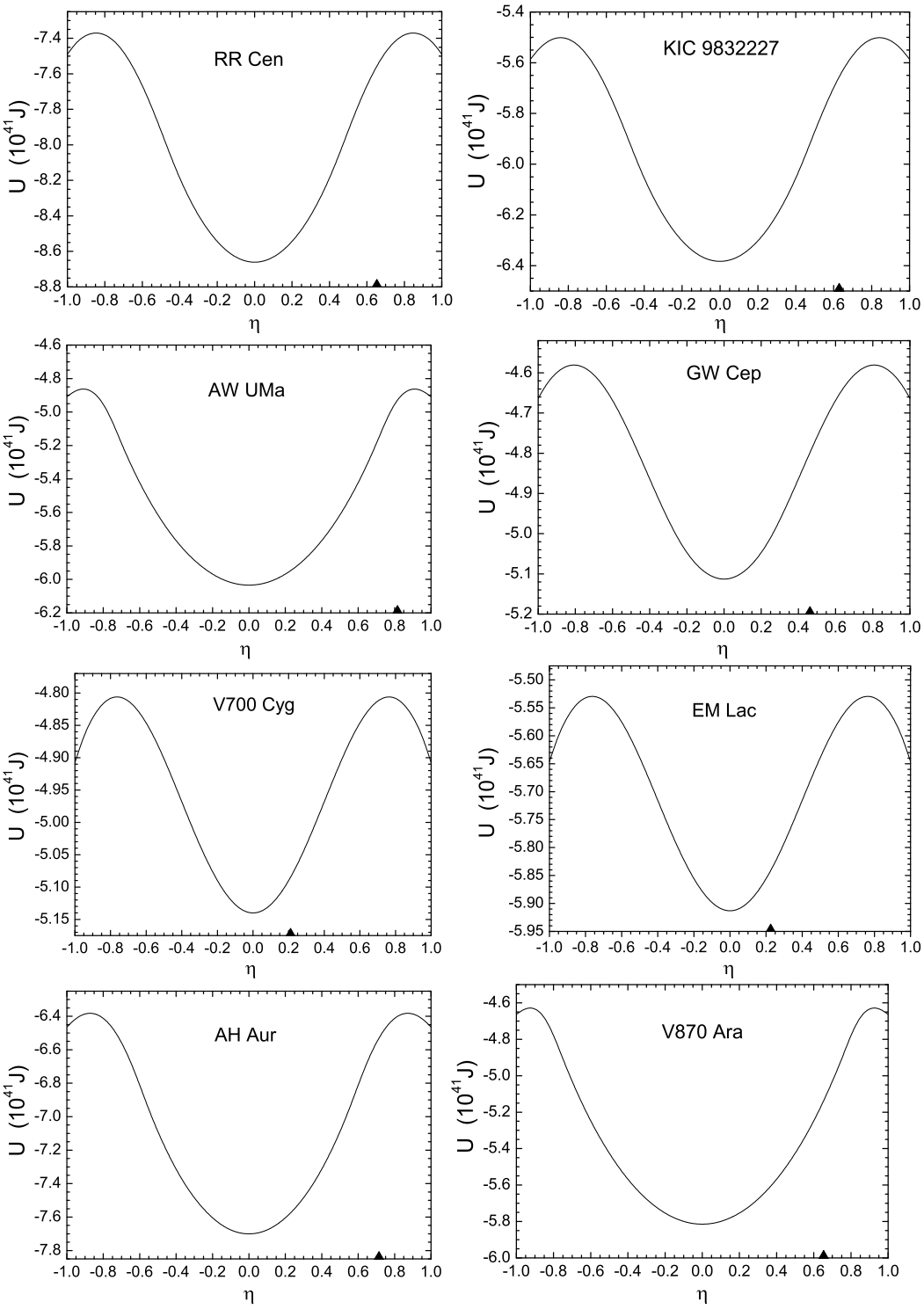

Figure 5. Driving potentials $U(\eta)$ calculated for the close binary stars indicated. The arrows indicate the values of η_i for the respective initial binary systems.

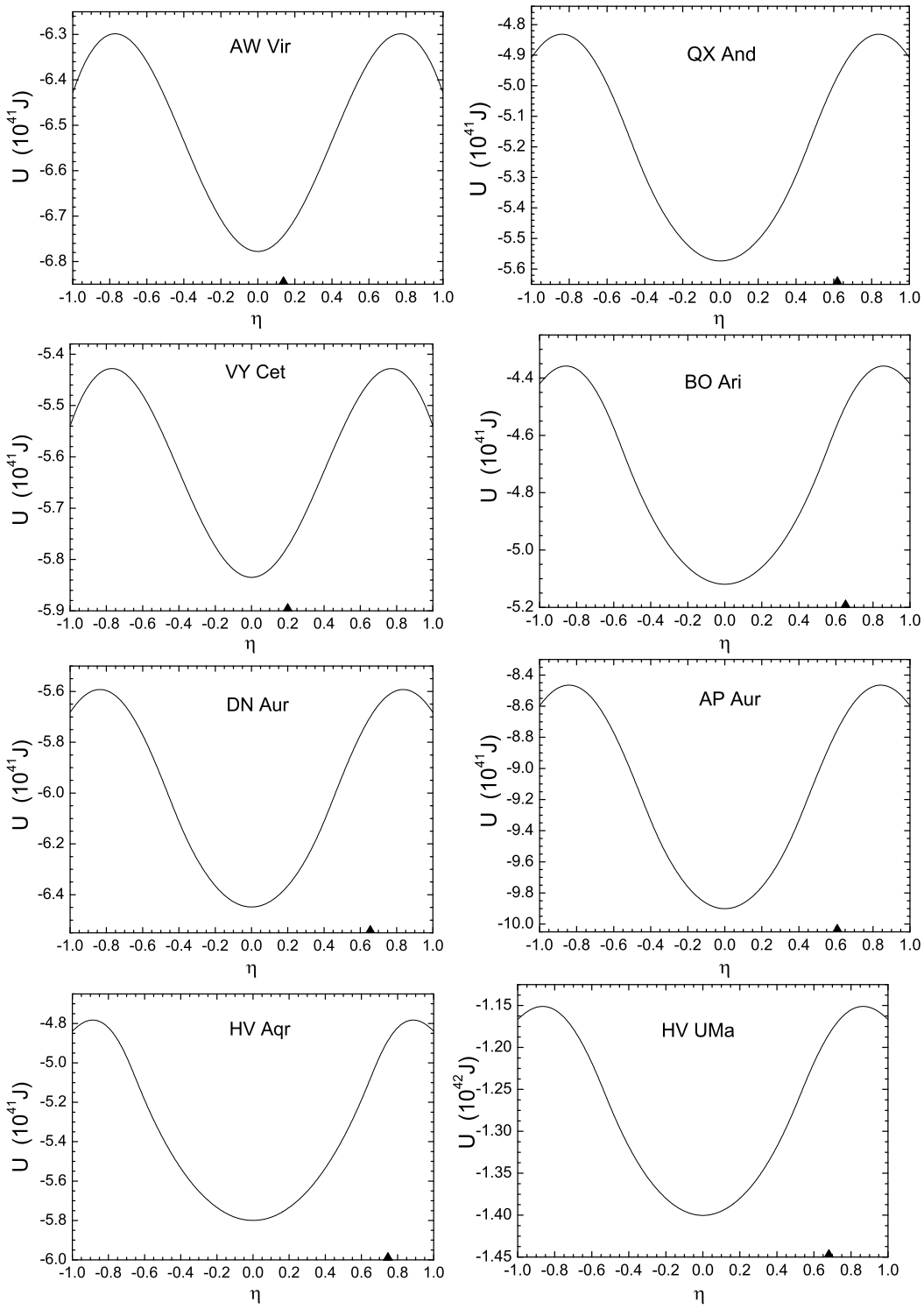

Figure 6. The same as in Figure 5, but for other close binary stars.

For the KIC 9832227, we studied the change of potential energy with the variations of the total mass M and orbital angular momentum L_i (Figure 7). We take effectively into consideration the losses of mass and angular momentum of the binary star during its evolution. As seen, simultaneous losses of M and L_i ($\Delta M \sim \Delta L_i$) by 20% or 50% weakly influence the features of potential energy. The decrease of M at fixed L_i affects stronger (the depth of the minimum in $U(\eta)$ decreases) but the evolution to the global symmetric minimum is still energetically favorable. So the related losses of M and L_i almost do not influence the symmetrization of the system.

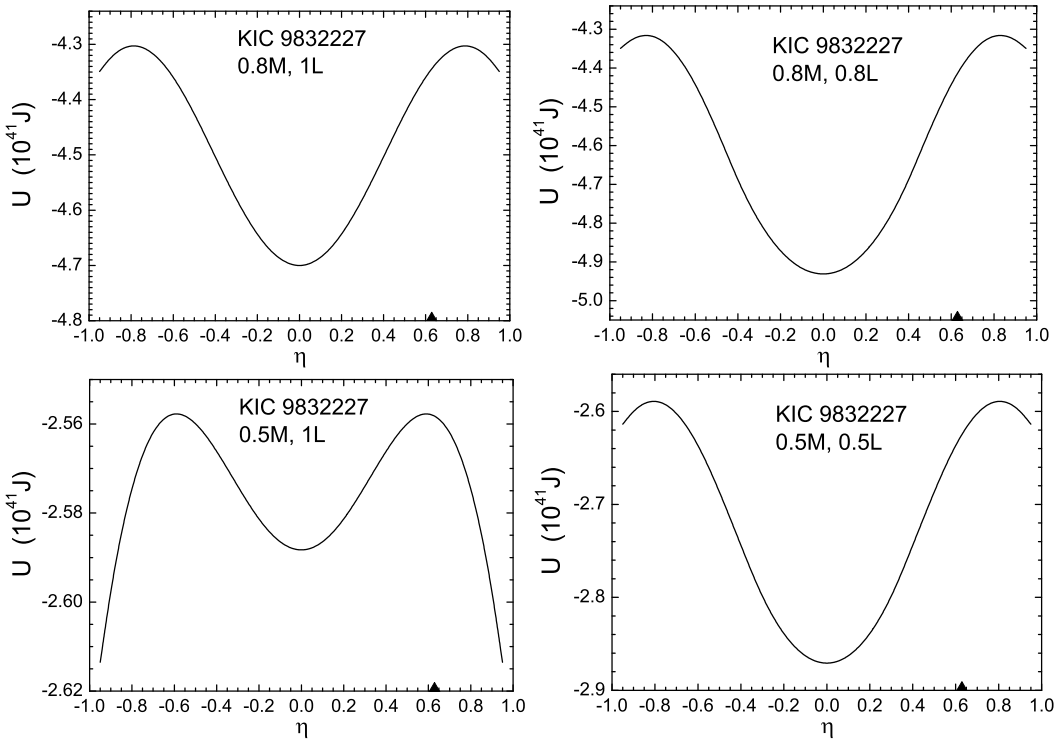

Figure 7. Calculated total potential energies U vs η for the binary star KIC 9832227. The notation (0.8 M, 1 L), (0.5 M, 1 L), (0.8 M, 0.8 L), and (0.5 M, 0.5 L) means that the calculations are performed with the losses of the total mass M and orbital angular momentum $L = L_i$ by (20%, 0%), (50%, 0%), (20%, 20%), and (50%, 50%), respectively. The arrows show the corresponding initial η_i for binary stars.

3.2. Close Binary Galaxies

In the calculations, the observational data from the catalog of isolated galaxy pairs [24] are employed: the linear diameters of galaxies, $A_{25}(1i, 2i) = 2R_{1i,2i}$; the projection of the linear distance X between the components of binary galaxies; and the total orbital mass M of pairs. In the close binary galaxies considered, the average relative distance $r_{mi} = \frac{4}{\pi}X$ between the galaxies is commensurate with the sum of the radii of these galaxies [24]. Matter transfer between the galaxies in a binary system is closely related to their radii and relative distance. If $M_{1i,2i} = MR_{1i,2i}^{5/2}/\left(R_{1i}^{5/2} + R_{2i}^{5/2}\right)$ at $n = 2/5$, then $\eta_i = \left(R_{1i}^{5/2} - R_{2i}^{5/2}\right)/\left(R_{1i}^{5/2} + R_{2i}^{5/2}\right)$. For the systems shown in ref. [24], $\alpha < \alpha_{cr} = \frac{25}{8}\beta$; therefore, the potential energy has a symmetric barrier at $\eta = \pm\eta_b$ and a minimum at $\eta = \eta_m = 0$. There is a similarity of the driving potentials $U(\eta)$ for macroscopic binary galaxies and stars to microscopic dinuclear systems [29,36,37].

Di-galaxies differ by r_{mi} and $R_{1i,2i}$, and, correspondingly, by the potential energy dependencies. In Figures 8 and 9, the driving potentials $U(\eta)$ are presented versus η for the close elliptic, spiral, and elliptic-spiral di-galaxy systems. For systems shown, except binary galaxy 272 [24], $\alpha < \alpha_{cr} = \frac{25}{8}\beta$ and, thus, there are potential barriers at $\eta = \pm\eta_b$ and a minimum at $\eta = \eta_m = 0$. The barrier in η appears from the interplay between the total gravitational energy $U_1 + U_2$ of the galaxies and the galaxy–galaxy interaction potential V. Note that the driving potentials $U(\eta)$ for the di-galaxy systems look like the driving potentials for the close binary stars and the microscopic dinuclear systems [29,30,36,37].

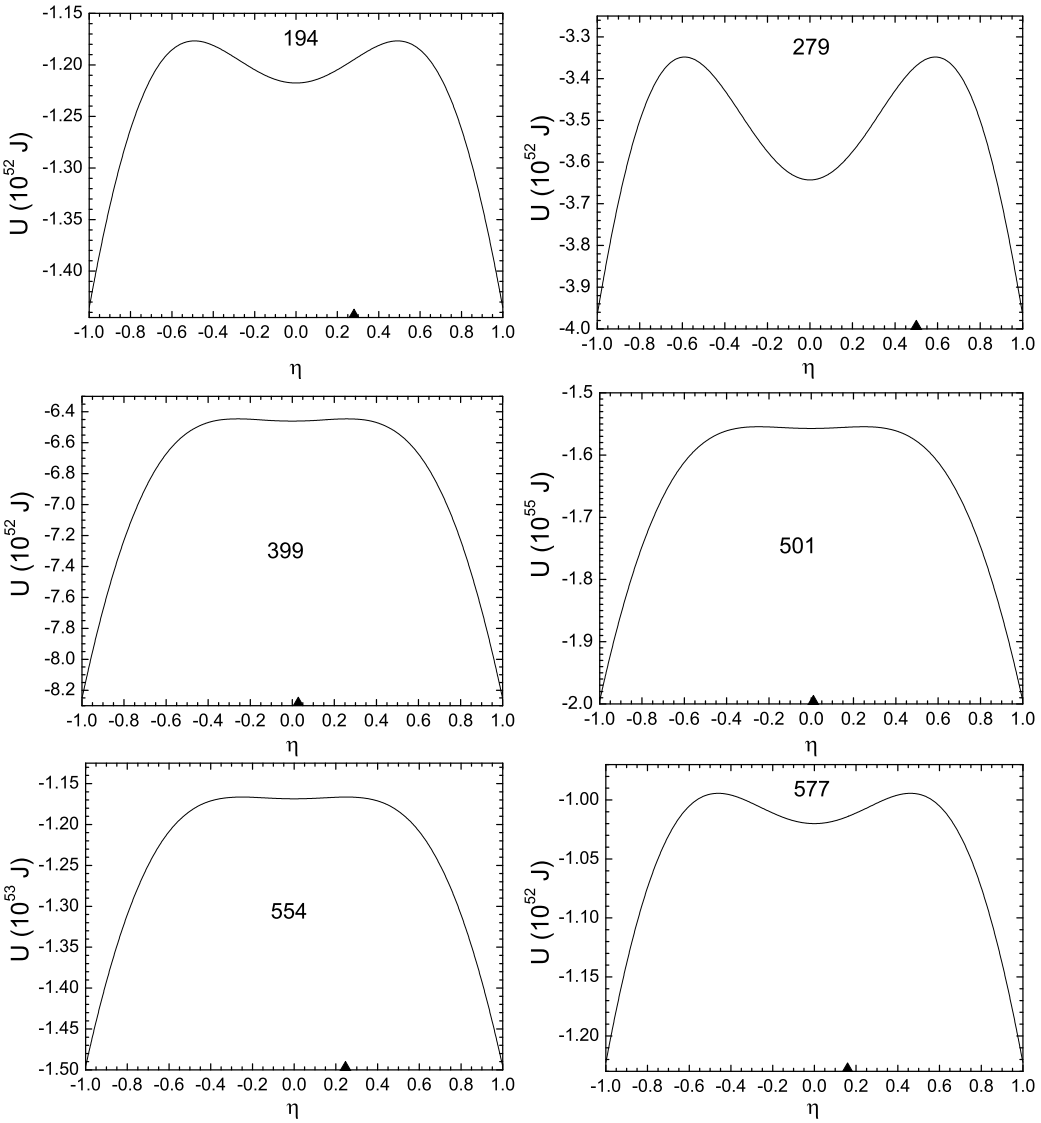

Figure 8. Calculated total potential energies U vs. η for the indicated (numbers) close binary elliptic galaxies at $n = 2/5$. The numbers are serial numbers of binary galaxies in the catalog of isolated pairs of galaxies [24]. The arrows show the corresponding initial η_i for binary galaxies.

An important question is to what extent the calculated results depend on the choice of the parameter n. The dependencies of the potentials calculated with $n = 2/3$ and $n = 2/5$ are qualitatively the same, except that the ratio $U(\eta = \eta_b)/U(\eta = 0)$ increases with n. So all binary systems considered evolve to the symmetric configurations independently of n.

The evolution path of a close binary galaxy depends on its initial mass asymmetry $\eta = \eta_i$. If the original di-galaxy is asymmetric with $|\eta_i| < \eta_b$, then its evolution in η to the global minimum at $\eta = 0$ is energetically favorable, that is, to form a symmetric di-galaxy system. The matter of a heavy galaxy can move freely to a light one enforcing symmetrization of di-galaxy without additional energy. This symmetrization leads to the decrease in potential energy U, thus transforming the potential energy into the internal kinetic energy. For example, for the close elliptic binary galaxies 194 (η_i = 0.28), 279 (η_i = 0.50), and 554 (η_i = 0.25) [24], the internal energies of galaxies increase during symmetrization by the amount $\Delta U = U(\eta_i) - U(\eta = 0) = 2 \times 10^{50}$, 3×10^{51}, and 2×10^{50} J, respectively (see Figures 8 and 9, and Tables 2–4). As found, most of the close binary galaxies are asymmetric and their symmetrization leads to the release of a large amount of energy (see Tables 2–4).

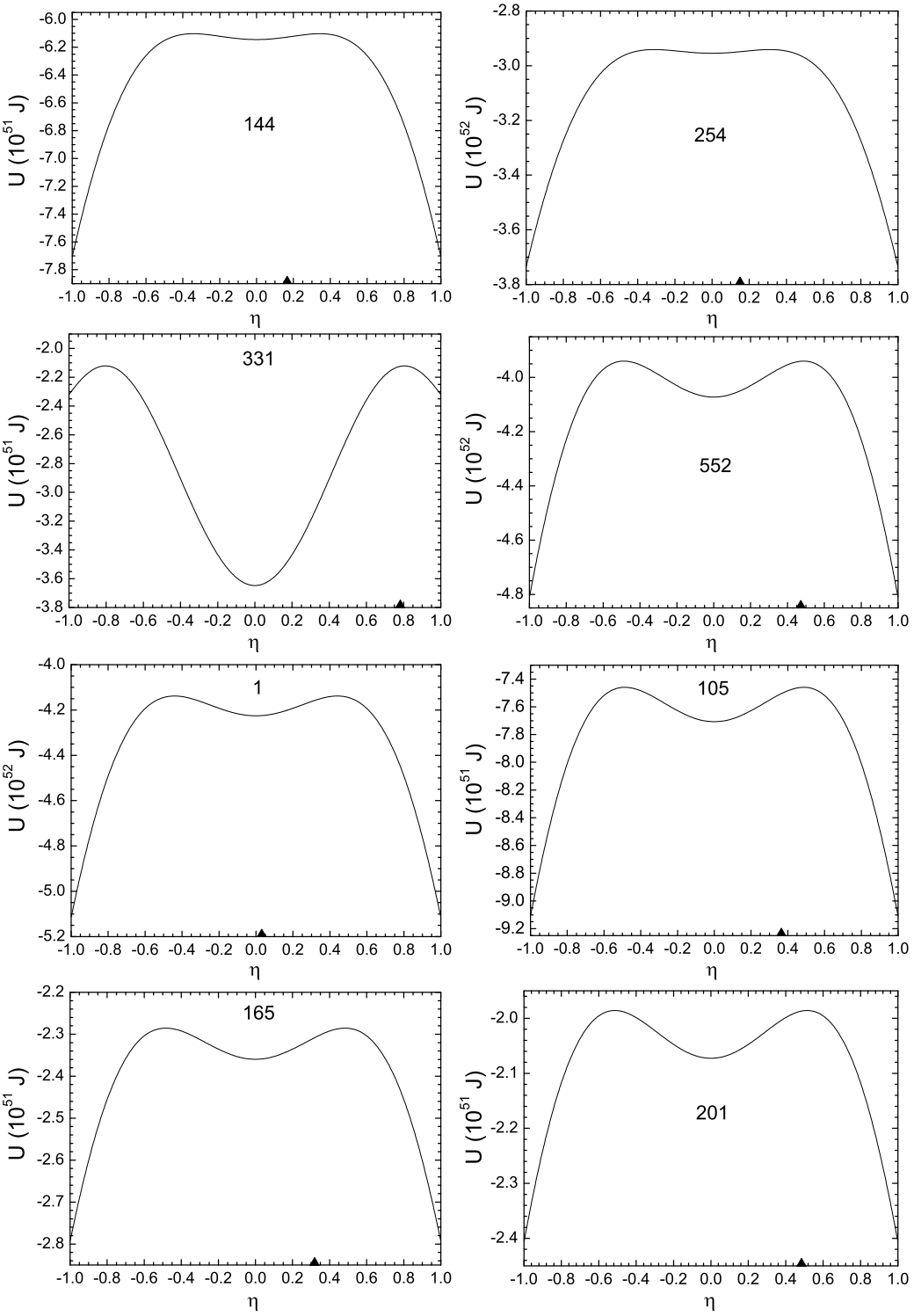

Figure 9. The same as in Figure 8 but for the close binary elliptic-spiral and spiral galaxies indicated.

If $|\eta_i| > \eta_b$ or $\eta_b = 0$, the di-galaxy system is unstable to evolve towards a more asymmetric system; thus, one galaxy "swallows" another. The matter flows freely from a light galaxy to a heavy one. This process leads to energy release. Representative examples of this mode of evolution are three close spiral binary galaxies, namely the galaxies 206 ($|\eta_i| = 0.45$, $\eta_b = 0.34$), 243 ($|\eta_i| = 0.31$, $\eta_b = 0.07$), and 439 ($|\eta_i| = 0.63$, $\eta_b = 0.56$) [24], respectively, for which $|\eta_i| > \eta_b$ (Table 4).

The binary galaxy with $|\eta_i| < \eta_b$ can merge only by overcoming the barrier at $\eta = +\eta_b$ or $\eta = -\eta_b$. With decreasing ratio α/β, the value of this barrier $B_\eta = U(\eta_b) - U(\eta_i)$

increases. Since the values of B_η are quite large for the systems with $|\eta_i| < \eta_b$ in Tables 2–4, asymmetrization of the di-star system due to thermal diffusion in η is strongly suppressed. Indeed, very asymmetric close binary galaxies with $|\eta_i| > \eta_b$ are rarely observed. This imposes restrictions on the asymmetric configurations with $|\eta| > \eta_b$ of the di-galaxy systems. There can not be a stable di-galactical system with a very light galaxy.

If the value of α becomes larger than α_{cr}, the minimum in $U(\eta)$ disappears, the inverted U-shaped potential appears with a maximum at $\eta = 0$, and the di-galaxy asymmetrization breaks the system finally apart. Hence, with increasing mass asymmetry, two constituents of the binary galaxy move away from each other to form two separate galaxies. The spiral binary galaxy 272 (see Table 4) is a good candidate to trace such evolution.

As found in our calculations, the double galaxy undergos either symmetrization or asymmetrization, depending on the original mass asymmetry. Asymmetrization may cause a merger process, but if the critical mass asymmetry is reached, the system is driven apart and forms two isolated galaxies with a changed mass ratio. This scenario can be considered an incomplete merger.

So the source of expansion of a binary galaxy is the transfer of matter from a lighter component to a heavier one. A necessary and sufficient condition for this is the fulfillment of the inequality

$$r_{mi} > \frac{0.15\left(R_{1i}^{5/2} + R_{2i}^{5/2}\right)^{22/5}}{R_{1i}^5 R_{2i}^5}.$$

The mechanism presented can be generalized for multiple galaxies, groups of galaxies, and galaxy associations.

4. Origin Of Orbital Period Change in Contact Binary Stars

As found, the orbital period of W-type overcontact binary GW Cep ($q = M_{1i}/M_{2i} = 0.37$, $\eta_i = 0.46$) decreases with time [39–41]. For the overcontact binaries VY Cet ($q = 0.67$, $\eta_i = 0.20$) and V700 Cyg ($q = 0.65$, $\eta_i = 0.21$), cyclic oscillations were found to be superimposed on an increase in the secular period. This effect was explained either by strong external perturbation, i.e., by a close-by third object, or by the magnetic activity cycles. For the EM Lac ($q = 0.63$, $\eta_i = 0.23$) and AW Vir ($q = 0.76$, $\eta_i = 0.14$) binaries, the periods demonstrate secular increase. As concluded, the period variations in a W UMa-type binary star correlate with the mass ratio q and the mass M_{1i} of the primary component [39–41]. The lower the mass ratio q in binaries, the shorter the period.

Using the relation between L and r_m, we obtain the period $P_{\rm orb} = \frac{2\pi}{\omega_{orb}} = \frac{2\pi\mu r_m^2}{L}$ of orbital rotation with frequency $\omega_{\rm orb}$. At $r_m > r_t$ and $r_m \leq r_t$ as

$$P_{\rm orb}^{>} = 2\pi\left(\frac{r_m^3}{GM}\right)^{1/2} \tag{24}$$

and

$$P_{\rm orb}^{<} = 2\pi\left(\frac{r_t^3}{GM}\right)^{1/2}, \tag{25}$$

respectively. As seen, at initial $|\eta_i| < |\eta_b|$ and $r_m > r_t$ ($r_m \leq r_t$), the system moves towards the symmetric configuration and, correspondingly, η decreases, r_m decreases (r_t increases), and finally, $P_{\rm orb}^{>}$ decreases ($P_{\rm orb}^{<}$ increases) [31,32].

For the KIC 9832227 system ($|\eta_i| = 0.63$), matter is transferred from a heavy star to a light one, the relative distance $r_m > r_t$ between two stars and the period $P_{\rm orb}^{>}$ of the orbital rotation decrease. The evolution in η pushes the system to the touching configuration ($r_m = r_t$) at some critical mass asymmetry $|\eta| = |\eta_t| \approx 0.45$ (Figure 10). Further evolution in η leads to a configuration with partial overlap ($r_m < r_t$) of stars. So at $|\eta| \leq |\eta_t|$ the period $P_{\rm orb}^{<}$ slightly increases because $P_{\rm orb}^{<} \sim r_t^{3/2}$ and r_t increases with decreasing η. Thus,

if the system reaches the point $\eta = \eta_t$ and partial overlap, the period abruptly changes. A similar period behavior is shown in Figure 10 for the other contact binaries considered.

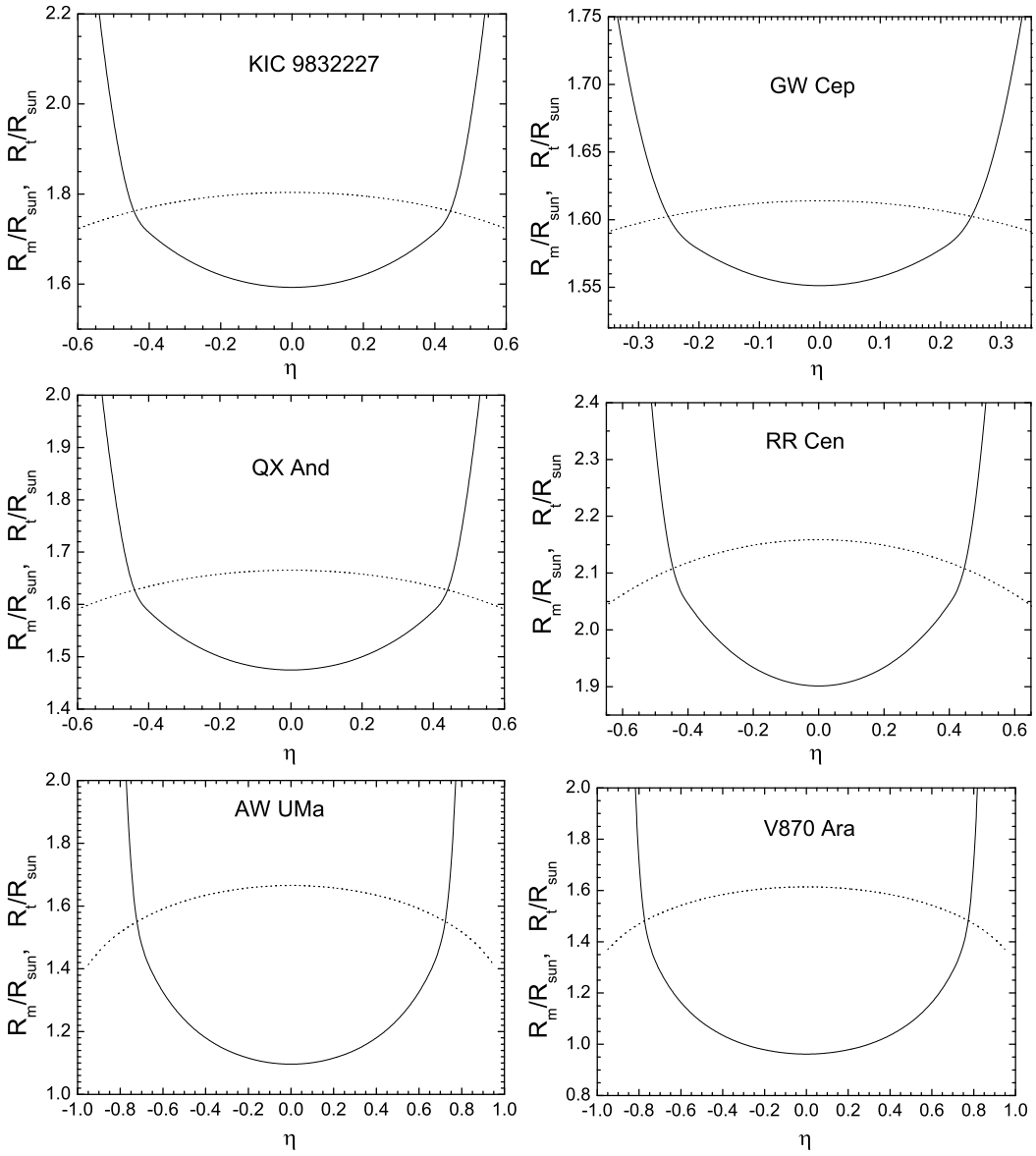

Figure 10. The calculated relative $r_m = R_m$ (solid lines) and touching $r_t = R_t = R_1 + R_2$ (dashed lines) distances between the components of di-stars indicated in the units of the Sun radius $R_{sun} = R_\odot$ vs. η.

For the binary GW Cep ($|\eta_i| = 0.46$), $|\eta_i| > |\eta_t|$, the system moves towards the symmetry and the orbital period decreases. For almost symmetric EM Lac ($|\eta_i| = 0.23$) and AW Vir ($|\eta_i| = 0.14$) binaries, $|\eta_i| < |\eta_t|$ and their periods increase. As found, the variations in the period of W UMa-type binary star correlate with the evolution towards a global symmetric minimum. At the low mass ratio q or the large η_i, the binaries usually demonstrate a decreasing period because $|\eta_i| > |\eta_t|$ ($r_m > r_t$), while the periods in systems with larger q (small η_i) increase because $|\eta_i| < |\eta_t|$ ($r_m < r_t$).

5. Stability of Macroscopic Binary Systems

The Regge theory turned out to be very influential in the development of elementary-particle physics [45–49]. As shown in the application of Regge's ideas to astrophysics, the spins of planets and stars are well described by the Regge-like law for a sphere ($S \sim M^{4/3}$),

while the spins of galaxies and clusters of galaxies obey the Regge-like law for a disk ($S \sim M^{3/2}$) [25,34,50–53]. Unlike semi-phenomenological approaches, these expressions contain only fundamental constants and do not depend on any established empirical quantities [25,34,50–53]. In Refs. [25,34,50–53], a cosmic analog of the Chew–Frautschi plot with two important cosmological Eddington and Chandrasekhar points was also constructed.

The Darwin instability effect can be studied in a binary star or galaxy by using the well-known model of Refs. [25,34,50–53] based on the Regge theory. The total angular momentum $\mathbf{J}_{\rm tot}$ of a binary system is the sum of the orbital angular momentum $\mathbf{L}$ and the spins $\mathbf{S}_k$ ($k = 1, 2$) of individual components:

$$\mathbf{J}_{\rm tot} = \mathbf{L} + \mathbf{S}_1 + \mathbf{S}_2. \tag{26}$$

The values of $J_{\rm tot}$ and S_i are expressed using the Regge-like law for stars and planets ($l = 3$) or galaxies ($l = 2$):

$$J_{\rm tot} = \hbar \left(\frac{M}{m_p} \right)^{(1+l)/l} \tag{27}$$

and

$$S_k = \hbar \left(\frac{M_k}{m_p} \right)^{(1+l)/l}, \tag{28}$$

where $\hbar$, m_p, M_k (k =1,2), and $M = M_1 + M_2$ are the Planck constant, masses of proton and astrophysical objects (planets, stars, or galaxies), and the total mass of the system, respectively. The maximum (L and $S_1 + S_2$ are antiparallel) and minimum (L and $S_1 + S_2$ are parallel) orbital angular momenta are

$$L_{\rm max} = J_{\rm tot} + S_1 + S_2 \tag{29}$$

and

$$L_{\rm min} = J_{\rm tot} - S_1 - S_2, \tag{30}$$

respectively. Using the coordinate η instead of masses M_1 and M_2 [33] and Equations (28)–(30), we derive

$$\frac{S_1 + S_2}{L_{\rm min}} = \frac{(1+\eta)^{(1+l)/l} + (1-\eta)^{(1+l)/l}}{2^{(1+l)/l} - (1+\eta)^{(1+l)/l} - (1-\eta)^{(1+l)/l}}, \tag{31}$$

$$\frac{S_1 + S_2}{L_{\rm max}} = \frac{(1+\eta)^{(1+l)/l} + (1-\eta)^{(1+l)/l}}{2^{(1+l)/l} + (1+\eta)^{(1+l)/l} + (1-\eta)^{(1+l)/l}}. \tag{32}$$

At $\eta = 0$ (the symmetric binary system), we have

$$\frac{S_1 + S_2}{L_{\rm min}} = \frac{1}{2^{1/l} - 1} > 1 \tag{33}$$

and

$$\frac{S_1 + S_2}{L_{\rm max}} = \frac{1}{2^{1/l} + 1} > \frac{1}{3}.$$

For the symmetric ($\eta = 0$) binary star (planet) and binary galaxy, $(S_1 + S_2)/L_{\rm max} \approx 0.44$ and 0.41, respectively.

At $\eta = 1$, we have

$$\frac{S_1 + S_2}{L_{\rm min}} \to \infty$$

and

$$\frac{S_1 + S_2}{L_{\max}} = \frac{1}{2}.$$

As follows from these expressions, for very asymmetric binaries, the ratios $(S_1 + S_2)/L_{\max,\min}$ are almost independent of l. According to ref. [20], the Darwin instability occurs when the binary mass ratio is very small [$q = M_2/M_1 < 0.1$] or the mass asymmetry is very large [$\eta = (1-q)/(1+q) > 0.82$]. As seen in Figure 11, the ratios $(S_1 + S_2)/L_{\max}$ and $(S_1 + S_2)/L_{\min}$ continuously increase with $|\eta|$. Since these ratios are larger than $1/3$, all possible binary stars (planets) or binary galaxies, independently of their mass asymmetry η, have the Darwin instability ($S_1 + S_2 \geq \frac{1}{3}L$) [19] and, thus, should merge. However, the observations do not confirm this, which probably means that there is no the Darwin instability effect in such binary systems and, accordingly, the mechanism of merger has a different origin and should be revealed. Since the spins of planets, stars, galaxies, and clusters of galaxies are well described by the Regge theory [25,34,50–53], we can be sure of the correctness of this conclusion.

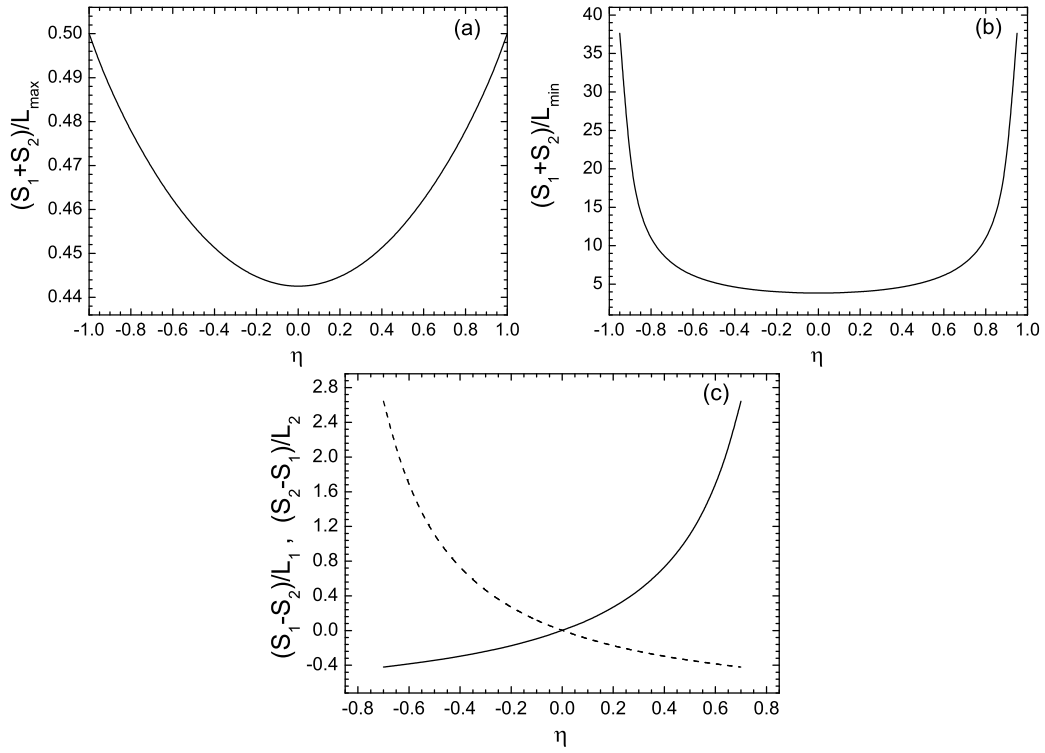

Figure 11. The calculated ratios $(S_1 + S_2)/L_{\max}$ (**a**), $(S_1 + S_2)/L_{\min}$ (**b**), $(S_1 - S_2)/L_2$ [solid line] (**c**), and $(S_2 - S_1)/L_1$ [dashed line] (**c**) as functions of mass asymmetry at $l = 3$. In the cases of antiparallel spins (**c**), $L_1 = J_{\text{tot}} + S_1 - S_2$ and $L_2 = J_{\text{tot}} - S_1 + S_2$.

Note that in the cases of antiparallel spins with $L_1 = J_{\text{tot}} + S_1 - S_2$ and $L_2 = J_{\text{tot}} - S_1 + S_2$ (Figure 11), the ratios $|S_2 - S_1|/L_1$ and $|S_1 - S_2|/L_2$ are larger than $1/3$ in the asymmetric binaries with $|\eta| \geq 0.5$.

As seen in Figure 12, the dependencies of $L_{\max}$, $L_{\min}$, L_1, and L_2 on η are different. The matter transfer can increase or decrease the orbital angular momentum. For example, at $\eta \to 0$ the binary system has smaller $L = L_{\max}$. The observations of L versus η may be useful to distinguish the difference between the orientations of orbital and spin momenta.

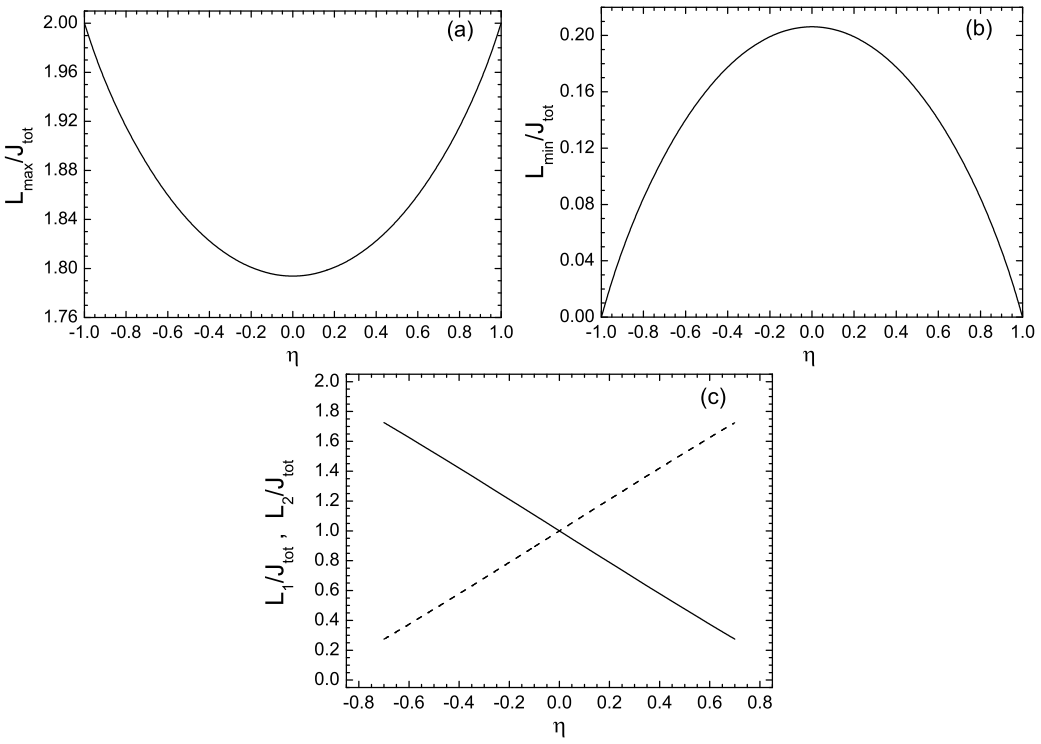

Figure 12. The calculated ratios $L_{\max}/J_{\rm tot}$ (**a**), $L_{\min}/J_{\rm tot}$ (**b**), $L_2/J_{\rm tot}$ [solid line] (**c**), and $L_1/J_{\rm tot}$ [dashed line] (**c**) as functions of mass asymmetry at $l = 3$.

Employing Equations (26)–(28) and the results of refs. [29,31,32], we obtain new analytical formulas for the relative distance between the components of the binary

$$\begin{aligned} r_m &= \frac{ML^2}{GM_1^2M_2^2} = \frac{\hbar^2 M}{GM_1^2M_2^2}\left[\left(\frac{M}{m_p}\right)^{(1+l)/l} + \epsilon_1\left(\frac{M_1}{m_p}\right)^{(1+l)/l} + \epsilon_2\left(\frac{M_2}{m_p}\right)^{(1+l)/l}\right]^2 \\ &= \frac{2\hbar^2}{Gm_p^3}\left(\frac{M}{2m_p}\right)^{(2-l)/l}\frac{\left[2^{(1+l)/l} + \epsilon_1(1+\eta)^{(1+l)/l} + \epsilon_2(1-\eta)^{(1+l)/l}\right]^2}{\left[1-\eta^2\right]^2} \end{aligned} \tag{34}$$

at $r_m \geq r_t$ and

$$\begin{aligned} r_m &= \left(\frac{\hbar M g^3}{GM_1^2M_2^2}\right)^{1/4}\left[M_1^l + M_2^l\right]^{3/4}\left[\left(\frac{M}{m_p}\right)^{(1+l)/l} + \epsilon_1\left(\frac{M_1}{m_p}\right)^{(1+l)/l} + \epsilon_2\left(\frac{M_2}{m_p}\right)^{(1+l)/l}\right]^{1/2} \\ &= \left(\frac{2\hbar m_p^{3n-3}g^3}{G}\right)^{1/4}\left(\frac{M}{2m_p}\right)^{(2+[3n-1]l)/l}\left[(1+\eta)^n + (1-\eta)^n\right]^{3/4} \\ &\times \frac{\left[2^{(1+l)/l} + \epsilon_1(1+\eta)^{(1+l)/l} + \epsilon_2(1-\eta)^{(1+l)/l}\right]^{1/2}}{\left[1-\eta^2\right]^{1/2}} \end{aligned} \tag{35}$$

at $r_m < r_t$. One can similarly derive the formulas for the orbital rotation period

$$\begin{aligned} P_{\rm orb} &= 2\pi\left(\frac{r_m^3}{GM}\right)^{1/2} = \frac{2\pi\hbar^3 M}{G^2M_1^3M_2^3}\left[\left(\frac{M}{m_p}\right)^{(1+l)/l} + \epsilon_1\left(\frac{M_1}{m_p}\right)^{(1+l)/l} + \epsilon_2\left(\frac{M_2}{m_p}\right)^{(1+l)/l}\right]^3 \\ &= \frac{4\pi\hbar^3}{G^2m_p^5}\left(\frac{M}{2m_p}\right)^{(3-2l)/l}\frac{\left[2^{(1+l)/l} + \epsilon_1(1+\eta)^{(1+l)/l} + \epsilon_2(1-\eta)^{(1+l)/l}\right]^3}{\left[1-\eta^2\right]^3} \end{aligned} \tag{36}$$

at $r_m \geq r_t$ and

$$\begin{aligned} P_{\rm orb} &= 2\pi\left(\frac{r_{\rm t}^3}{GM}\right)^{1/2} = 2\pi\left(\frac{g^3\left[M_1^n + M_2^n\right]^3}{GM}\right)^{1/2} \\ &= 2\pi\left(\frac{g^3 m_p^{3n-1}}{2G}\right)^{1/2}\left(\frac{M}{2m_p}\right)^{(3n-1)/2}\left[(1+\eta)^n + (1-\eta)^n\right]^{3/2} \end{aligned} \quad (37)$$

at $r_m < r_t$ [31,32]. The values $\epsilon_1 = \epsilon_2 = 1$ and $\epsilon_1 = \epsilon_2 = -1$ correspond to the cases of antiparallel and parallel, respectively, orbital and spin angular momenta. In the cases of antiparallel spins, $\epsilon_1 = -\epsilon_2 = 1$ and $\epsilon_1 = -\epsilon_2 = -1$. The observation data result in the relationship $R_k = M_k^l/g$ between the radius and mass of the star, where $n = \frac{2}{3}$ and $g = M_\odot^{2/3}/R_\odot$ [6] and the galaxy, where the value of n depending on mass is in the interval $\left[\frac{2}{5}, \frac{2}{3}\right]$ [24,30]. As seen in Figure 13, at $r_m > r_t$,

$$r_m^d = R_m^d = \frac{\left[2^{(1+l)/l} + \epsilon_1(1+\eta)^{(1+l)/l} + \epsilon_2(1-\eta)^{(1+l)/l}\right]^2}{\left[1-\eta^2\right]^2}$$

or r_m decreases with $|\eta|$ and, finally,

$$P_{\rm orb}^d = \frac{\left[2^{(1+l)/l} + \epsilon_1(1+\eta)^{(1+l)/l} + \epsilon_2(1-\eta)^{(1+l)/l}\right]^3}{\left[1-\eta^2\right]^3}$$

or $P_{\rm orb}$ decreases. At $r_m > r_t$ (Figure 13), the dependence of $P_{\rm orb}$ as a function of mass asymmetry has similar behavior at antiparallel and parallel orbital and spin angular momenta. In the case of antiparallel spins with $L_1 = J_{\rm tot} + S_1 - S_2$ ($L_2 = J_{\rm tot} - S_1 + S_2$) and $M_1 \geq M_2$, the values of r_m and $P_{\rm orb}$ decrease (increase) with η decreasing from 1 to 0 (Figure 14). At $r_m \leq r_t$ (Figure 15), the value of

$$P_{\rm orb}^d = \left[(1+\eta)^n + (1-\eta)^n\right]^{3/2}$$

or $P_{\rm orb}$ increases with decreasing $|\eta|$ and does not depend on mutual orientations of orbital momentum and spins. In contrast, the distance

$$R_m^d = \left[(1+\eta)^n + (1-\eta)^n\right]^{3/4}\frac{\left[2^{(1+l)/l} + \epsilon_1(1+\eta)^{(1+l)/l} + \epsilon_2(1-\eta)^{(1+l)/l}\right]^{1/2}}{\left[1-\eta^2\right]^{1/2}}$$

or r_m depends on the orientations of orbital momentum and spins. As seen in Figure 15, the dependencies of R_m^d on η at different spins have various behaviors.

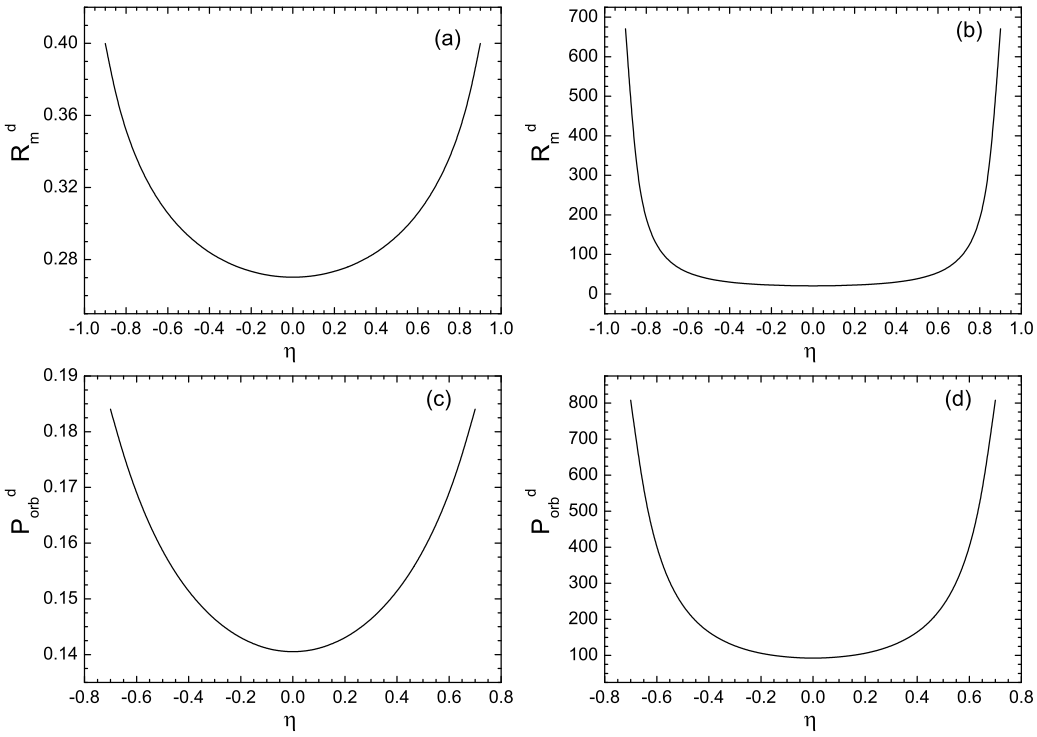

Figure 13. The calculated dimensionless relative distances $r_m^d = R_m^d$ (**a**,**b**) and orbital rotation periods $P_{\rm orb}^d$ (**c**,**d**) as functions of η at $r_m > r_t$ ($r_m = R_m$, $r_t = R_t$) and $l = 3$. The plots (**a**,**c**) and (**b**,**d**) correspond to the systems with the parallel and antiparallel orbital angular momentum and spin.

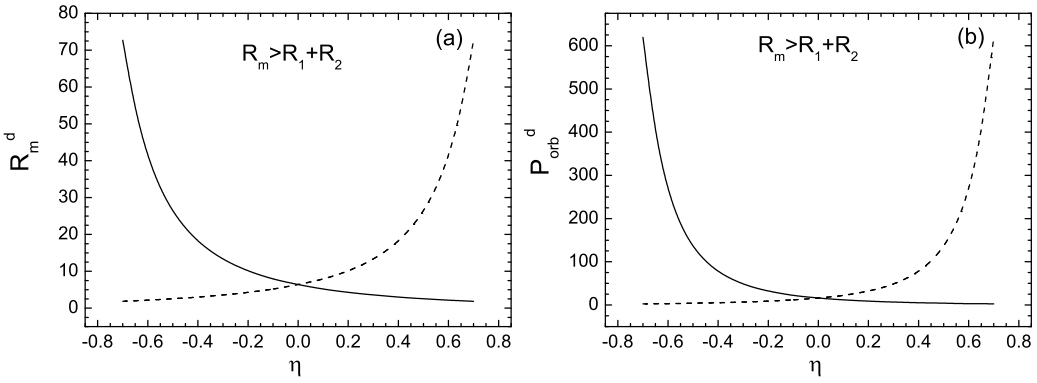

Figure 14. The calculated dimensionless relative distance $r_m^d = R_m^d$ (**a**) and orbital rotation period $P_{\rm orb}^d$ (**b**) as functions of η in the cases of antiparallel spins with $L_1 = J_{\rm tot} + S_1 - S_2$ (dashed line) and $L_2 = J_{\rm tot} - S_1 + S_2$ (solid line), $l = 3$, and $r_m > r_t$ ($r_m = R_m$, $r_t = R_t$).

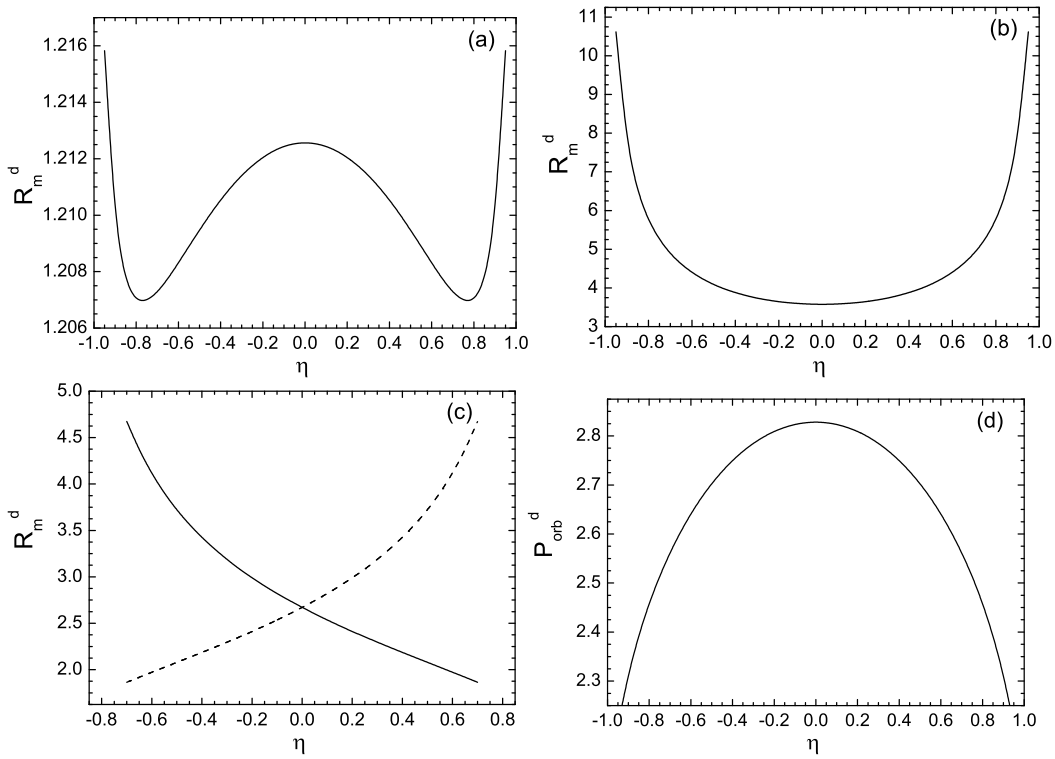

Figure 15. The calculated dimensionless $r_m^d = R_m^d$ (**a**–**c**) and $P_{\rm orb}^d$ (**d**) as functions of η at $r_m \le r_t$ ($r_m = R_m$, $r_t = R_t$), $l = 3$, and $n = 2/3$. The plots (**a**,**b**) correspond to the system with the parallel and antiparallel orbital angular momentum and spin, respectively. In the plot (**c**), the cases of antiparallel spins with $L_1 = J_{\rm tot} + S_1 - S_2$ (dashed line) and $L_2 = J_{\rm tot} - S_1 + S_2$ (solid line) are presented. Note that the value of $P_{\rm orb}^d$ does not depend on the orientations of the orbital momentum and spins.

6. Possibility of Formation of Binary Cosmic System From Single Cosmic Object

6.1. Close Binary Stars

For transition from a single star with mass M and potential energy $U(\eta = \pm 1)$ to an asymmetric or almost symmetric binary star with $|\eta| < |\eta_b|$, the system should overcome the height barrier $B_f = U(|\eta| = \eta_b) - U(|\eta| = 1)$ at $\eta = \pm\eta_b$. The values of B_f are too large (see Figures 5 and 6 and Table 1) to allow the single star to be transformed into a binary star with $|\eta| < |\eta_b|$ due to thermal fluctuations [35]. Thus, the fission in η (matter transfer from a heavier star to a lighter one) cannot be the origin of binary stars. Our conclusion is consistent with that of ref. [26,28]. If the fission hypothesis mentioned is not valid, then the only possible conclusion can be the assumption of a common origin of the components of a binary star from a pre-stellar state of matter [28]. Thus, some stars likely arise during the formation of stellar groups in the form of pairs, triplets, quartets, etc. The observed excess of binary stars in the stellar associations suggests that these binary stars transform into ordinary binary stars after leaving the associations [28].

6.2. Close Binary Galaxies

In the galactic systems from Tables 2–4, and Figures 8 and 9, the fission barriers B_f in η are too high to form almost symmetric binary and asymmetric galaxies with $|\eta| < |\eta_b|$ from the single galaxy via thermal fluctuations of η [35]. So we arrive at the same conclusion as in the case of fission of single stars.

7. On Evolution of Compact Binary Black Holes

The general view is that compact binary systems consisting of white dwarfs, neutron stars, and black holes eventually merge as a result of gravitational wave radiation, as recently observed with the LIGO and Virgo interferometers [14]. The process of merging is still insufficiently studied. We are going to add a few aspects highlighting the role of

matter transfer in binary black holes (BBH) [34], which are certainly a special class of objects. The presence of the event horizon restrains the flow of mass between two cores of BBH. At a speculative level, quantum tunneling as the Hawking radiation [54] may play a faint, most likely insignificant role due to not yet received firm confirmation. However, a BBH is usually embedded in a cloud of remnant matter left over from the progenitor stars. Therefore, a BBH should always be considered together with the surrounding accretion disk. The material of that disk may serve as the matter transfer between two cores by the so-called *sloshing effect*, as illustrated by the hydrodynamical calculations in ref. [55].

In order to understand the possibility of matter exchange in a BBH system, we consider the potential energy of a BBH as a function of η. The possibility of matter transfer based on the potential energy of a BBH system should always be understood together with its accretion disk. In addition to the BBH's own extremely strong gravitational fields, the potential energy contains the interaction potential between two black holes. Being well aware of the strong gravitational fields, we use Newtonian mechanics because, at a distance, post-Newtonian effects can alter the binary potential by no more than 25% [55], which will not affect the overall BBH properties. General relativity becomes of course, essential at separations close to touching.

The total potential energy

$$U = U_1 + U_2 + V_{1R} + V_{2R} + V \tag{38}$$

of a BBH is given by the sum of the potential U_k ($k = 1, 2$) and rotational energies V_{kR} ($k = 1, 2$) of two nonzero spin black holes, and the black hole–black hole interaction potential V. The energy of the black hole "k" is

$$U_k = -\frac{GM_k^2}{R_k}, \tag{39}$$

where G, M_k, and R_k are the gravitational constant, mass, and radius of the black hole, respectively. The rotation energy of a black hole is

$$V_{kR} = \frac{S_k \Omega_k}{2} = \frac{M_k c^2}{2}, \tag{40}$$

where $S_k = M_k R_k c$ and $\Omega_k = c/R_k$ are the spin and rotational frequency of the black hole "k", respectively.

The radius of the event horizon (distance from the gravitating mass M_k at which the particle velocity is equal to c) [25,34,50–53]

$$R_k = \frac{GM_k}{c^2} \tag{41}$$

is derived from the energy conservation law for a particle with mass m: $-GM_k m/R_k + mc^2 = 0$, where mc^2 is the sum of the kinetic $mc^2/2$ and rotation $mc^2/2$ energies. The derivation of the radius R_k is based on classical mechanics and the Newtonian law of gravity. In ref. [56], the expression $R_k = 2GM_k/c^2$ was also obtained for a non-rotating black hole. Using Equations (39) and (41), we obtain

$$U_k = -M_k c^2. \tag{42}$$

Due to the rotation of two black holes around the common center of mass, the black hole–black hole interaction potential $V(r)$ contains, together with the gravitational potential V_G, the kinetic energy of orbital rotation V_R:

$$V(r) = V_G + V_R = V_G + \frac{L^2}{2\mu r^2} = V_G + \frac{\mu v_r^2}{2}, \tag{43}$$

where L, $v_r = (GM[2/r - 1/r_m])^{1/2}$ and r_m are the orbital angular momentum of a BBH, the speed and the semi-major axis of an elliptical relative orbit, respectively. At $r \geq r_t$, the black hole–black hole interaction potential is defined as in Equation (8). From the conditions $\partial V/\partial r|_{r=r_m} = 0$ and $\partial^2 V/\partial r^2|_{r=r_m} > 0$, we find the relative equilibrium distance between two black holes corresponding to the minimum of V (see Equation (10)). The total angular momentum $J = GM^2/c$ of a BBH [25,34,50–53] is assumed to be conserved during the conservative matter transfer and the orbital angular momentum of a BBH is

$$L = J - S_1 - S_2 = \frac{G(M^2 - M_1^2 - M_2^2)}{c}. \tag{44}$$

Here the orbital momentum and spins are parallel and the value of L is minimal. Employing Equations (10) and (44), we derive the expression

$$r_m = \frac{4GM}{c^2}. \tag{45}$$

As seen, the larger M, the larger r_m. Since $r_m/(R_1 + R_2) = 4$, the separation of the components increases at $M_1 \to M_2$. From Equations (8), (43) and (45) we obtain the simple formula

$$V(r_m) = -\frac{GM_1M_2}{2r_m} = -\frac{M_1M_2c^2}{8M} = -\frac{\mu c^2}{8} \tag{46}$$

for the interaction potential. The value of $V(r_m)$ depends only on the reduced mass μ and the velocity of light.

So using Equations (40), (42) and (46), we derive the final expression

$$U = -\frac{Mc^2}{2}\left(1 + \frac{M_1M_2}{4M^2}\right) = -\frac{Mc^2}{2}\left(1 + \frac{\mu}{4M}\right) \tag{47}$$

for the total potential energy of a BBH.

For the BBH considered, $v_r(r_m) = (GM/r_m)^{1/2} = c/2$ and with good accuracy, one can disregard relativistic effects and use the Newtonian law of gravity.

Employing the coordinate η instead of masses M_1 and M_2, we rewrite expressions (44) and (47) for the orbital angular momentum

$$L = \frac{GM^2}{2c}\left(1 - \eta^2\right) \tag{48}$$

and the total potential energy

$$U = -\frac{Mc^2}{2}\left(1 + \frac{1 - \eta^2}{16}\right). \tag{49}$$

Since the solution of the equation

$$\frac{\partial U}{\partial \eta} = \frac{Mc^2}{16}\eta = 0$$

leads to $\eta = \eta_m = 0$ and

$$\frac{\partial^2 U}{\partial \eta^2}|_{\eta=\eta_m} = \frac{Mc^2}{16} > 0,$$

the potential landscape has a global minimum at $\eta = \eta_m = 0$ for an arbitrary total mass M of a BBH (Figure 16). So the transfer of matter between the black holes in the BBH is energetically favorable and can occur to reach a global minimum. The initial asymmetric system is easily driven to the symmetric BBH. This conclusion does not depend on the

choice of parameters. The losses of the total mass and orbital angular momentum do not affect symmetrization of a BBH. The transfer of matter between two black holes becomes possible because they interact with their own extreme gravitational fields. However, the evolution of a BBH in η depends also on the parameter of inertia in this coordinate. Since the surfaces of two black holes are spaced $R_1 + R_2 < r_m$ from each other, the parameter of inertia in η is expected to be very large and, accordingly, prohibits symmetrization of a BBH.

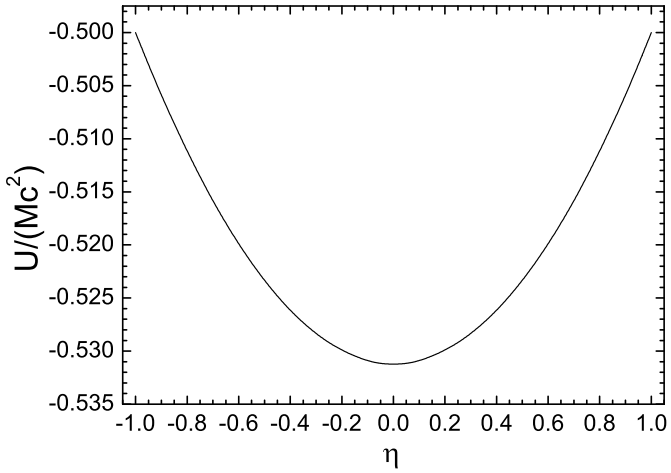

Figure 16. Dependence of potential energy of the BBH (49) on η.

Asymmetrization (the transfer of matter from a lighter component to a heavy one) of a BBH considered is energetically unfavorable, and, correspondingly, the merger channel in η is strongly suppressed. Thus, the question of the mechanism of the merger of two black holes and the origin of gravitational waves remains open [14].

At antiparallel orbital momentum and spins, the value of

$$L = J + S_1 + S_2 = \frac{G(M^2 + M_1^2 + M_2^2)}{c} \tag{50}$$

is maximal. For a BBH with this L,

$$U = -\frac{Mc^2}{2}\left(1 + \frac{(1-\eta^2)^3}{16(3+\eta^2)^2}\right) \tag{51}$$

and $r_m/(R_1 + R_2) \geq 36$, $v(r_m) = (GM/r_m)^{1/2} \leq c/6$, $\eta_m = 0$, $\partial^2 U/\partial\eta^2|_{\eta=\eta_m} > 0$, and all conclusions given above are also valid in this case. Comparing Figures 16 and 17, we can draw the same conclusions in the case when black holes in a BBH spin in the opposite directions.

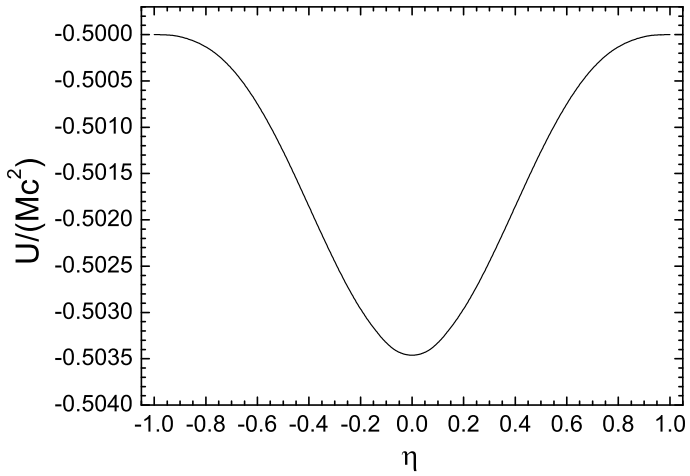

Figure 17. Dependence of potential energy of the BBH (51) on η.

8. Summary

The evolution of isolated binary stellar and galactic systems was considered in the framework of the approach originally formulated for the study of nuclear fusion reactions, thus combining scales that differ by many orders of magnitude. Despite the differences in details, the common aspects of macroscopic objects (di-star, di-galaxy, BBH) and microscopic dinuclear systems prevail. Both types of systems evolve along well-defined trajectories in the classical phase space. The conserved quantity is the total energy, that is, the Hamilton function, of a binary system. Using general arguments, we have shown that the conservation of energy is sufficient to fix the trajectory of a binary system in the landscape of potential energy determined by the masses of the objects and their interaction. Exploiting the stationarity of the total energy, the stability conditions were derived and investigated as a function of mass asymmetry. We emphasized that the interpretation of mass asymmetry as a collective coordinate has been successfully used to describe nuclear reactions, the cluster structure of nuclei, the decay of dinuclear systems, and the fusion of two heavy nuclei [36,37]. Here we have shown that this collective degree of freedom plays a comparably important role in space objects. In close di-star or di-galaxy systems, the coordinate η can govern the merger and symmetrization (due to the matter transfer) processes. An interesting aspect is that once η is determined, for example, by observation, it is possible to draw a conclusion about the stellar or galactic structure.

The new theoretical interpretation of a di-star or di-galaxy system is based on the fact that, after the formation, the lifetime of a binary system is long enough to reach equilibrium conditions in the mass asymmetry coordinate. Therefore, we could conclude that the system will be included in the sample of all binary and single configurations with the probability depending on the potential energy of this configuration. For the systems considered, $\alpha < \alpha_{cr}$ and there are potential barriers at $\eta = \pm\eta_b$ and minimum at $\eta = \eta_m = 0$. So two distinct evolution scenarios arise: if $|\eta_i| < \eta_b$, the system is driven to the symmetric configuration (towards a global minimum of the potential landscape). However, if $|\eta_i| > \eta_b$, the binary system evolves towards the mono-object system. All the considered asymmetric close binary systems, with the exception of the di-star α Cr B and di-galaxies 206, 243, 272, 439, satisfy the condition $|\eta_i| < \eta_b$ and a symmetrization process occurs in these systems. The loss of the total mass and orbital angular momentum has little effect on the process of symmetrization. The merger of the binary stars, including the KIC 9832227, and binary galaxies considered is energetically unfavorable. The formation of a single object from the binary system ($|\eta_i| < \eta_b$) by thermal diffusion in the mass asymmetry coordinate is strongly suppressed.

Symmetrization of a binary system ($|\eta_i| < \eta_b$) due to the matter transfer is one of the important sources of conversion of gravitational energy into other types of energy in the universe. For example, in the cases of compact binary stars and compact binary galaxies,

the released energies are about $10^{39} - 10^{41}$ and $10^{48} - 10^{52}$ J, respectively. Symmetrization of a binary system will lead to close objects with equal masses, temperatures, luminosities, and radii, which are observable quantities. During the process of mass-symmetrization, the channels of binary decay in the relative coordinate are closed. The central result of the approach reviewed is that stable binary systems exist only at $|\eta| < \eta_b = 2^{-1/2}$ ($M_1/M_2 < (1 + 2^{1/2})^2 \simeq 6$) because otherwise, the stars are getting closer to merging. Thus, di-stars or di-galaxies with $|\eta| > \eta_b$ can not exist for long enough. Indeed, binary systems with a large ratio M_1/M_2 are very rare objects in the universe.

Asymmetrization (the transfer of matter from a lighter component to a heavy one) is equivalent to incomplete merging. Asymmetrization is also the origin of the expansion of a binary galaxy. The separation of components from each other is represented as an analog of the expansion of the universe within a binary system. The condition under which the asymmetrization process is realized depends mainly on the relative distance between the components of binary systems and their linear dimensions.

For contact di-stars, changes in the orbital period can be well explained by evolution in η towards symmetry. We predicted that the decrease and increase in orbital periods are associated, respectively, with the non-overlapping ($|\eta_i| > |\eta_t|$, $r_m \geq R_1 + R_2$) and overlapping ($|\eta_i| < |\eta_t|$, $r_m < R_1 + R_2$) stages of a binary star during its symmetrization. Thus, observing the change of periods allows us to distinguish between these two stages of a di-star.

Based on calculations of potential energy, we have demonstrated that the mass asymmetry coordinate (matter transfer) is useful for analyzing the transformation of a single star (galaxy) into a binary star (galaxy). Mass ejection from a single star could create a binary star in the mass asymmetry coordinate. However, the barrier preventing symmetrization in η is quite high. So the formation of asymmetric and almost symmetric di-star or di-galaxy systems from the respective mono-star or mono-galaxy by thermal overcoming of barriers in the driving potential (the diffusion process in η) is hardly possible. Binary stars (galaxies) with a mass ratio $M_1/M_2 > 6$ evolve to more asymmetric configurations and are rather unstable with respect to the decay in the relative distance. Thus, matter ejection from a single star is either captured back or escapes, which is consistent with the findings of refs. [26,28]. Thus, it is possible to assume a common origin of the components of a binary star (galaxy) from the pre-stellar (pre-galactic) state of matter.

Based on the Regge-like laws [25,34,50–53], we demonstrated that all possible binary stars (planets) or binary galaxies, regardless of their mass asymmetry, satisfy the Darwin instability condition ($S_1 + S_2 \geq \frac{1}{3}L$), which contradicts observations. This output is not sensitive to model parameters. Therefore, we should look for another mechanism that triggers the merger of binary contact components. Employing the Regge-like laws, we derived new analytical formulas for the relative distance and orbital rotation period of the binary system, which depend on the total mass M, mass asymmetry η, and the fundamental constants G, $\hbar$, and m_p.

Employing Newton's law of gravity and considering the BBH potential energy as a function of η, we have shown the possibility of transferring matter between black holes in a BBH. The evolution of an asymmetric BBH to a symmetric one ($\eta = \eta_m = 0$) is energetically favorable. Although black holes have their own strong gravitational fields, the transfer of matter in BBH occurs due to the energy of interaction between two black holes. A BBH does not send any signals during its evolution. Perhaps the result of this evolution can be indirectly observed.

Symmetrization of a BBH leads to a decrease of U, thus converting the potential energy into internal kinetic energy. For example, for the BBH $4M_\odot + 2M_\odot$ ($\eta_i = 0.33$) and $36M_\odot + 29M_\odot$ ($\eta_i = 0.11$), the internal energies of black holes increase during symmetrization by the amount $\Delta U = U(\eta_i) - U(\eta = 0) = Mc^2\eta_i^2 \approx 10^{47}$ J. So the BBH is also the source of thermal energy. The transfer of matter from a lighter component to a heavier one (the merger of black holes in a BBH) is not an energetically advantageous process, and, thus, the question of the origin of gravitational waves remains open.

Within the presented model, we can also perform dynamic calculations of the evolution of a binary system in η. For example, we can calculate the relaxation time (symmetrization) and the asymmetrization time. In addition to the total potential energy, it is also necessary to calculate the mass parameter and the coefficient of friction for this coordinate. However, this extension of the model is the subject of future research.

Acknowledgments: We are grateful to Alexis Diaz-Torres and Avas Khugaev for fruitful discussions.

Author Contributions: All authors contributed equally to this investigation. All authors have read and agreed to the published version of the manuscript.

Funding: This work was partially supported by the Alexander von Humboldt-Stiftung (Bonn).

Institutional Review Board Statement: Not applicable.

Informed Consent Statement: Not applicable.

Data Availability Statement: Not applicable.

Conflicts of Interest: The authors declare no conflict of interest.

References

1. Kopal, Z. *Close Binary Systems*; Shapman and Hall Ltd.: London, UK, 1978.
2. Shore, S.N.; Livio, M.; van den Heuvel, E.P.J. *Interacting Binaries*; Springer: Berlin/Heidelberg, Germany, 1994.
3. Hilditch, R.W. *An Introduction to Close Binary Stars*; Cambridge University Press: Cambridge, UK, 2001.
4. Boyarchuk, A.A. *Mass Transfer in Close Binary Stars*; Taylor and Francis: London, UK; New York, NY, USA, 2002.
5. Eggleton, P.P. *Evolutionary Processes in Binary and Multiple Stars*; Cambridge University Press: Cambridge, UK, 2006.
6. Vasiliev, B.V. Astrophysics and Astronomical Measurement Data. Available online: http://astro07.narod.ru (accessed on 1 January 2022).
7. Cherepashchuk, A.M. *Close Binary Stars, Volumes I and II*; Fizmatlit: Moscow, Russia, 2013. (In Russian)
8. Molnar, L.A.; Van Noord, D.M.; Kinemuchi, K.; Smolinski, J.P.; Alexander, C.E.; Cook, E.M.; Jang, B.; Kobulnicky, H.A.; Spedden, C.J.; Steenwyk, S.D. Prediction of a red nova outburst in kic 9832227. *arXiv* **2017**, arXiv:1704.05502.
9. Kulkarni, S.R.; Ofek, E.O.; Rau, A.; Cenko, S.B.; Soderberg, A.M.; Fox, D.B.; Gal-Yam, A.; Capak, P.L.; Moon, D.S.; Li, W.; et al. An unusually brilliant transient in the galaxy M85. *Nature* **2007**, 447, 458. [CrossRef] [PubMed]
10. Tylenda, R.; Hajduk, M.; Kamiński, T.; Udalski, A.; Soszyński, I.; Szymański, M.K.; Kubiak, M.; Pietrzyński, G.; Poleski, R.; Ulaczyk, K. V1309 Scorpii: merger of a contact binary. *Astron. Astrophys.* **2011**, *528*, A114. [CrossRef]
11. Soker, N.; Tylenda, R. Main-Sequence Stellar Eruption Model for V838 Monocerotis. *APJL* **2003**, *582*, L105. [CrossRef]
12. Sana, H.; de Mink, S.E.; de Koter, A.; Langer, N.; Evans, C.J.; Gieles, M.; Gosset, E.; Izzard, R.G.; Le Bouquin, J.-B.; Schneider, F.R.N.; et al. Binary Interaction Dominates the Evolution of Massive Stars. *Science* **2012**, *337*, 444. [CrossRef]
13. Kochanek, C.S.; Adams, S.M.; Belczynski, K. Stellar mergers are common. *MNRAS* **2014** , *443*, 1319. [CrossRef]
14. Abbott, B.P.; LIGO Scientific and Virgo Collaboration. Erratum: Tests of general relativity with gw150914. *Phys. Rev. Lett.* **2016**, *116*, 241102. [CrossRef] [PubMed]
15. Pejcha, O.; Metzger, B.D.; Tyles, J.G.; Tomida, K. Pre-explosion Spiral Mass Loss of a Binary Star Merger. *Astrophys. J.* **2017**, *850*, 59. [CrossRef]
16. Eggleton, P.P. Formation and Evolution of Contact Binaries. Available online: https://koreascience.kr/article/JAKO201218559656013.pdf (accessed on 1 January 2022).
17. Fabrycky, D.; Tremaine, S. Shrinking Binary and Planetary Orbits by Kozai Cycles with Tidal Friction. *Astrophys. J.* **2007**, *669*, 1298. [CrossRef]
18. Tokovinin, A.; Thomas, S.; Sterzik, M.; Udry, S. Tertiary companions to close spectroscopic binaries. *Astron. Astrophys.* **2006**, *450*, 681. [CrossRef]
19. Darwin, G.H. The determination of the secular effects of tidal friction by a graphical method. *Proc. R. Soc.* **1879**, *29*, 168.
20. Rasio, F.A. The Minimum Mass Ratio of W Ursae Majoris Binaries. *APJL* **1995**, *444*, L41. [CrossRef]
21. Stępień, K. Evolution of the progenitor binary of V1309 Scorpii before merger. *Astron. Astrophys.* **2011**, *531*, A18. [CrossRef]
22. D'Souza , M.C.R.; Motl, P.M.; Tohline, J.E.; Frank, J. Numerical Simulations of the Onset and Stability of Dynamical Mass Transfer in Binaries. *Astrophys. J.* **2006**, *643*, 381. [CrossRef]
23. Koenigsberger, G.; Moreno, E. Stability of Macroscopic Binary Systems. *Rev. Mex. Astron. Astrofis.* **2016**, *52*, 113.
24. Karachentsev, I.D. *Binary Galaxies*; Nauka: Moscow, Russia, 1987. (In Russian)
25. Muradian, R.M. The Regge law for heavenly bodies. *Phys. Part. Nucl.* **1997**, *28*, 471. [CrossRef]
26. Ambartsumian, V.A. On the origin of double stars. *Vistas Astron.* **1937**, *14*, 207. [CrossRef]
27. Ambartsumian, V.A.; Mirzoyan, L.V. An observational approach to the early stages of stellar evolution. *Natl. Acad. Sci. Armen.* **1947**, *84*, 317–330

28. Ambartsumian, V.A. *Vistas in Astronomy*; Beer, A., Ed.; Elsevier: Amsterdam, The Netherland, 1956; Volume 2.
29. Sargsyan, V.V.; Lenske, H.; Adamian, G.G.; Antonenko, N.V. From dinuclear systems to close binary stars: Application to mass transfer. *Int. J. Mod. Phys. E* **2018**, *27*, 1850063. [CrossRef]
30. Sargsyan, V.V.; Lenske, H.; Adamian, G.G.; Antonenko, N.V. Close Binary Galaxies: Application to Source of Energy and Expansion in Universe. *Int. J. Mod. Phys. E* **2019**, *28*, 1950031. [CrossRef]
31. Sargsyan, V.V.; Lenske, H.; Adamian, G.G.; Antonenko, N.V. Origin of the orbital period change in contact binary stars. *Int. J. Mod. Phys. E* **2019**, *28*, 1950044. [CrossRef]
32. Sargsyan, V.V.; Lenske, H.; Adamian, G.G.; Antonenko, N.V. From dinuclear systems to close binary stars and galaxies. *Phys. Atom. Nucl.* **2020**, *83*, 60.
33. Adamian, G.G.; Antonenko, N.V.; Lenske, H.; Sargsyan, V.V. Stability of Macroscopic Binary Systems. *Commun. Theor. Phys.* **2019**, *71*, 1335. [CrossRef]
34. Adamian, G.G.; Antonenko, N.V.; Lenske, H.; Sargsyan, V.V. On the evolution of compact binary black holes. *Int. J. Mod. Phys. E* **2020**, *29*, 2050094. [CrossRef]
35. Adamian, G.G.; Antonenko, N.V.; Lenske, H.; Sargsyan, V.V. On the possibility of formation of binary cosmic systems from the single cosmic objects. *Int. J. Mod. Phys. E* **2022**, *31*, 2250071. [CrossRef]
36. Adamian, G.G.; Antonenko, N.V.; Scheid, W. Clustering effects within the dinuclear model. in book. In *Clusters in Nuclei*; Lecture Notes in Physics; Beck, C., Ed.; Springer: Berlin, Germany, 2012; Volume 2.
37. Adamian, G.G.; Antonenko, N.V.; Zubov, A.S. Dinuclear systems in complete fusion reactions. *Phys. Part. Nucl.* **2014**, *45*, 848. [CrossRef]
38. Devries, R.M.; Clover, M.R. Coulomb potentials in heavy-ion interactions. *Nucl. Phys. A* **1975**, *243*, 528. [CrossRef]
39. Qian, S.-B. A possible relation between the period change and the mass ratio for W-type contact binaries. *Mon. Not. R. Astron. Soc.* **2001**, *328*, 635–644. [CrossRef]
40. Qian, S.-B. Are overcontact binaries undergoing thermal relaxation oscillation with variable angular momentum loss? *Mon. Not. R. Astron. Soc.* **2003**, *342*, 1260.
41. Yang, Y.-G.; Qian, S.-B. Deep, low mass ratio overcontact binary systems. XIV. A statistical analysis of 46 sample binaries. *Astron. J.* **2015**, *150*, 69.
42. Yakut, K.; Eggleton, P.P. Evolution of close binary systems. *Astrophys. J.* **2005**, *629*, 1055. [CrossRef]
43. Gazeas, K.; Stepien, K. Angular momentum and mass evolution of contact binaries. *Mon. Not. R. Astron. Soc.* **2008**, *390*, 1577.
44. Socia, Q.J.; Welsh, W.F.; Short, D.R.; Orosz, J.A.; Angione, R.J.; Windmiller, G.; Caldwell, D.A.; Batalha, N.M. KIC 9832227: Using Vulcan Data to negate the 2022 Red Nova merger prediction. *Astrophys. J. Lett.* **2018**, *864*, L32. [CrossRef]
45. Regge, T. Introduction to complex orbital momenta. *Nuovo Cim.* **1959**, *14*, 951. [CrossRef]
46. Collins, P.D.B. *An Introduction to Regge Theory and High Energy Physics*; Cambringe University Press: Cambringe, UK, 1977.
47. Barone, V.; Predazzi, E. *High-Energy Particle Diffraction*; Springer: Berlin/Heidelberg, Germany, 2002.
48. Chew, G.F.P.; Frautschi, S.C. Principle of Equivalence for all Strongly Interacting Particles within the S-Matrix Framework. *Phys. Rev. Lett.* **1961**, *7*, 394. [CrossRef]
49. Gribov, V.N. Partial waves with complex orbital angular momenta and the asymptotic behavior of the scattering amplitude. *Sov. Phys. JETP* **1961**, *14*, 1395.
50. Muradian, R.M. The Primeval Hadron—Origin of Stars Galaxies and Astronomical Universe. *Astrophys. Space Sci.* **1980**, *69*, 339. [CrossRef]
51. Muradian, R.M. On the origin of the rotation of galaxies in Ambartsumian's cosmogony. *Astrofiz* **1975**, *11*, 237. (In Russian)
52. Muradian, R.M. Cosmic numbers and the rotation of the metagalaxy. *Astrofiz* **1977**, *13*, 63. (In Russian)
53. Muradian, R.M. Origin of magnetic fields and superdense cosmogony. *Astrofiz* **1978**, *14*, 439. (In Russian)
54. Hawking, S.W. Black hole explosions? *Nature* **1974**, *248*, 30. [CrossRef]
55. Bowen, D.B.; Campanelli, M.; Krolik, J.H.; Mewes, V.; Noble, S.C. Electromagnetic Emission from Supermassive Binary Black Holes Approaching Merger. *Astrophys. J.* **2017**, *838*, 42.
56. Michell, J., VII. On the means of discovering the distance, magnitude, &c. of the fixed stars, in consequence of the diminution of the velocity of their light, in case such a diminution should be found to take place in any of them, and such other data should be procured from observations, as would be farther necessary for that purpose. *Phylosophical Trans. R. Soc.* **1784**, *74*, 35.